

We thank the reviewers for their constructive comments, suggestions, and corrections. This version has been largely improved owing to their helpful review. In our revision, we have addressed the reviewer's concerns. The following is a one-to-one response to their questions. Following the reviewers' suggestions, the major improvements in this revision are as follows.

- 1. We have reconstructed the paper to make it more concise. The presentation is polished throughout and more in-depth discussion is added. A large part of the paper is rewritten.*
- 2. We have added more details on the validations between the ozonesonde observations and GEOS-Chem simulations.*
- 3. More details are provided and discussed about GEOS-Chem, including the emission inventories, the tagged ozone simulations, and other issues raised by the reviewers.*
- 4. The trajectory analysis is improved in this revision. More discussions are added in this revision throughout section 3.3, in section 4.2, and in the conclusions (section 5).*

A manuscript with tracked changes is followed.

Response to Comments by Anonymous Referee #1

General Comments:

The authors provide a detailed analysis for the long-range transport of tropospheric O₃ from Africa to Asia. They indicated that African O₃ have important influences on free tropospheric O₃ over Asia, and the imported African O₃ peaks in winter because of the shifts of transport and emission patterns. I recommend the paper for publication after consideration of the points below.

1) The paper isn't concise enough for me. For example, Section 5 provides a summary for the transport and emission processes, which is actually a repeat of Section 4.2. In addition, considering the small contribution from SHAF (shown by Figure 4), it may not be necessary to have an individual section (Section 4.3) to discuss its influence.

Thanks for the comments and suggestions. We have reconstructed the paper to make it more concise. Section 5 in the last version has been removed. The presentation is polished throughout the paper and more in-depth discussion is added. We have reconstructed the section on the interhemispheric transport of ozone from SNAF and added more analyses in this section (now section 4.2). Therefore, we think it is better

to keep this section.

2) The discussion should be improved. The authors should explain why the seasonal variability of biogenic isoprene is so weak (Figure 6); and revise the discussion about the contributions from various sources (i.e. biogenic, biomass burning and lightning, Section 4.2).

Thanks for the points. In the last version, the color scale for the seasonal variation of biogenic isoprene in Figure 6 was not appropriate so that the seasonal variation was not shown apparently. We have edited the color scale so to better show the magnitude of the seasonal variation of biogenic isoprene (now Figure 8). The regional means of the seasonal variation of biogenic isoprene over Africa is shown in Figure 9, which shows large seasonality of biogenic emissions. The discussion about the contributions from various sources has been revised and discussed in more depth (now in section 3.3).

Specific Comments:

1: Line 147-149 Are the O₃ production and loss rates generated using the full-chemistry simulation with the current model settings or from other studies (Wang et al. 1998; Zhang et al. 2008)?

In this study, we generated the ozone production and loss rates from the full-chemistry simulation using the current model settings of GEOS-Chem v9-02. We have clarified this in this revision (see section 2.1).

2: Line 149-153 It would be better to show these regions as boxes in the map (e.g. Figure 5). It is difficult to imagine the regions just based on these lat/lon numbers.

Thanks for your suggestion. We have added Fig. 1 to show the definitions of the regions. The sites used in the GEOS-Chem validation and trajectory analysis are also shown in Fig. 1.

3: Line 155-157 Did the authors evaluate the possible influences from interannual

variations of meteorology on chemistry?

Thanks for the question. In this study, we focus on the impact of meteorology on the transport. Therefore, we keep the ozone production and loss rate fixed in one year and allow the meteorology to vary from year to year.

Yes, meteorology also affects chemistry. If keeping ozone production term constant, the meteorology influence on chemistry is ignored. We have pointed this out in this revision (section 2.1, the last 2nd paragraph). We have not directly evaluated this impact. Instead, we have tested if this impact will significantly alter our results. Therefore, we conduct a sensitivity test. First, we run GEOS-Chem in full chemistry mode to generate ozone production rate and loss frequency in other two different years. Years 2001 and 2004 are selected because these are years when the extreme anomalies of imported African ozone appear in Asia. In the two full chemistry simulations, we used the same anthropogenic and biomass burning emissions in 2005 but with the different meteorology in 2001 and 2004 respectively. Therefore, the differences in the ozone production rate and loss frequency data can be regarded as the meteorology influences on chemistry as the emissions are fixed. Then we use these two sets of daily ozone production and loss frequency to run the tagged ozone simulations for 20 years. First, we compare the 20-year mean of imported African ozone from these two runs with the default run in Fig.1. The differences of imported African ozone over Asia between three datasets are small, varying from -1 ppbv to 0.2 ppbv for most layers and months, although the differences are large in NH winter over the upper troposphere, reaching 1-3 ppbv.

Second, we compare the three datasets on the interannual variations of imported African ozone over Asia in Fig. 2. Indeed, there are differences between the three datasets. However, the interannual variations of the three simulations are similar and all positive correlated to the ITCZ. This sensitivity test suggests that our treatment is robust in capturing the variation of ozone transport from Africa to Asia from year to year.

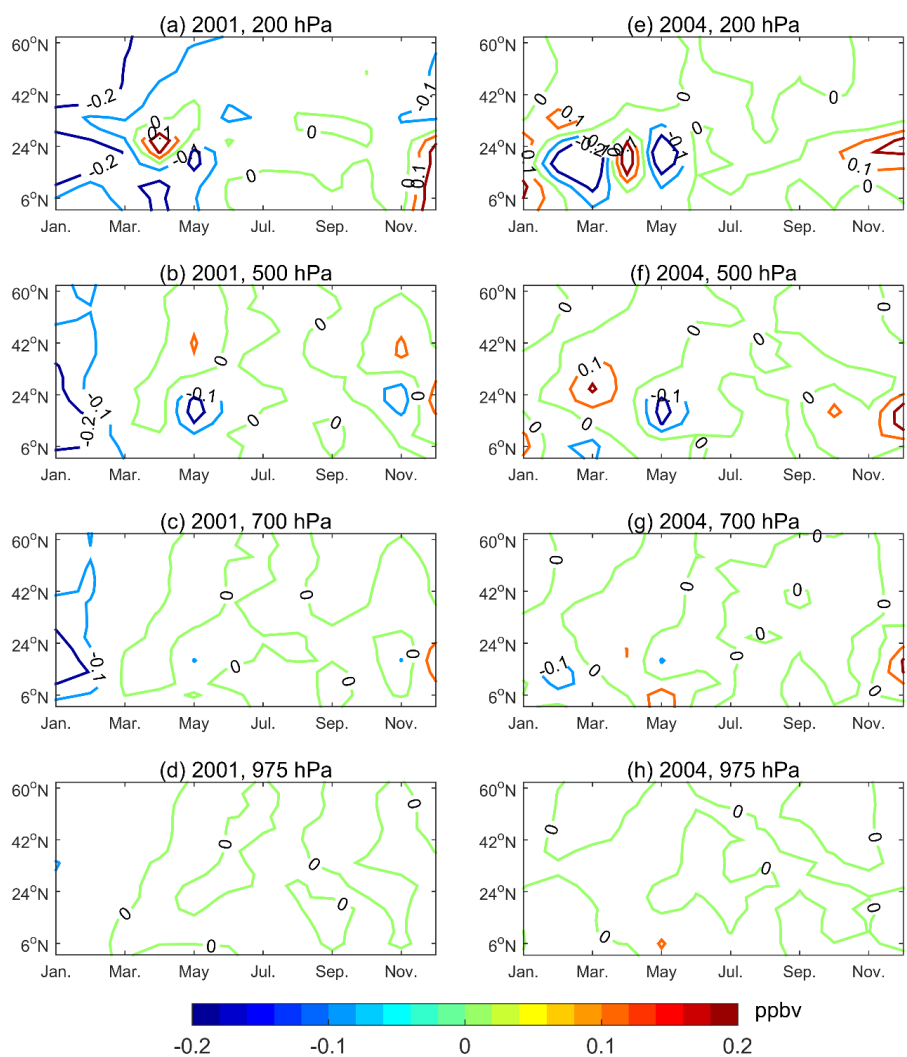


Figure S1. The differences of imported African ozone over Asia between the 2005 and the 2001 datasets (1st col.) and between the 2005 and the 2004 dataset (2nd col.). The values are averaged over 60-145°E from 1987 to 2006. Associated with the three datasets, the ozone production and loss data are generated with the same emissions but different meteorology in 2001, 2004, and 2005.

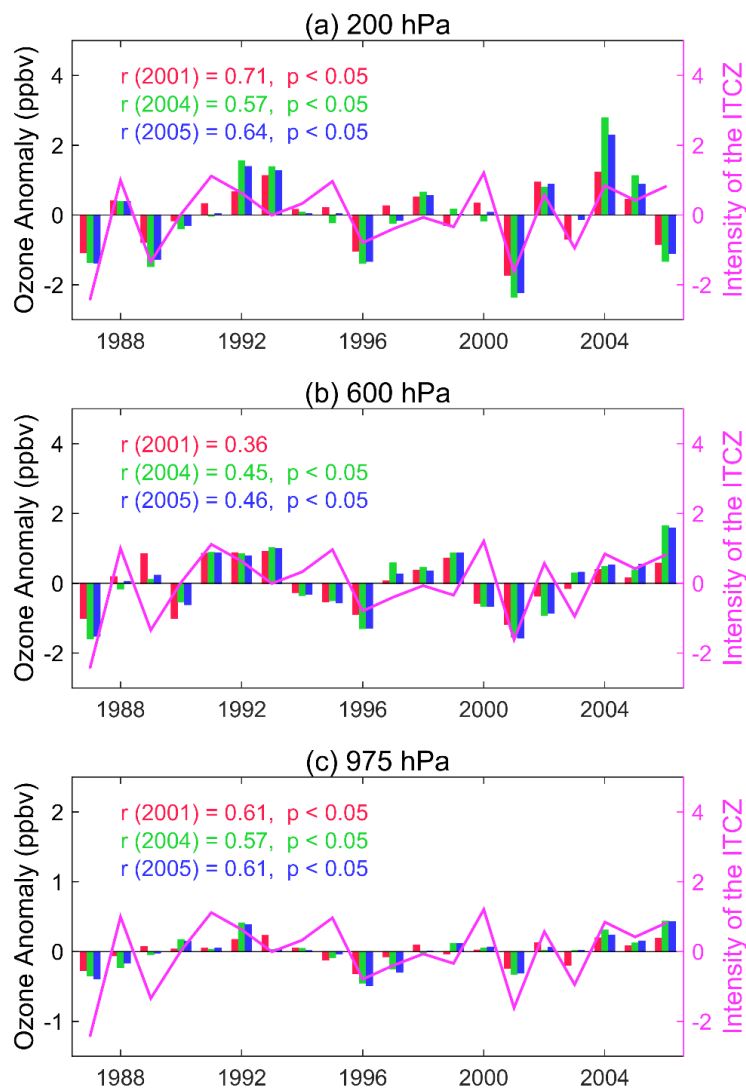


Figure 2. The interannual variations of the anomaly of imported African ozone over Asia simulated using the three sets of ozone production and loss data at (a) 200 hPa, (b) 600 hPa, and (c) 975 hPa in January. Associated with the three datasets, the ozone production and loss data are generated with the same emissions but different meteorology in 2001, 2004, and 2005.

4: Line 166-167 Is there any other station available? Why are these three stations selected?

GEOS-Chem simulations have been validated with ozonesonde data extensively, for example, in North America (Zhang et al., 2008; Zhu et al., 2017b), Europe (Kim et al., 2015), and East Asia (Wang et al., 2011; Zhu et al., 2017a; Zhu et al., 2017b). However, few studies have validated the simulations in Africa. We specifically validate the performance of GEOS-Chem over Africa for an enhanced confidence on our analysis. These three stations are selected for their representative locations and relative long records in Africa. In this version, the ozone data from three ozonesonde stations in India are added to compare with the GEOS-Chem simulations. In addition, the Tropospheric Emission Spectrometer (TES) satellite observations are compared with the GEOS-Chem simulation in the middle troposphere shown in the supplementary file (Fig. S6).

5: Section 2.3 Is the meteorological data the same as used by the HYSPLIT model? If they are the same, it would be better to combine Section 2.2 with Section 2.3.

The meteorological data are the same as what are used by the HYSPLIT model. The two parts have been combined into Section 2.3.

6: Line 237-239 The influence of African O₃ to south America across Atlantic is discussed, but isn't shown in the Figure. It could be better to remove the discussion about the transatlantic transport here.

The discussion about the transatlantic transport here has been removed.

7: Line 262-269 Although may not be necessary to explain, I am just curious about the reason for the discrepancy between western and eastern Africa.

In general, the latitudinal position of ITCZ follows the rotation of the sun. In eastern Africa, the seasonal migration of ITCZ with latitude is more symmetrical around the equator, while in western Africa, the migration is limited (Collier and Hughes, 2011). The seasonal migration of the ITCZ in western Africa is complicated. Generally, in

NH summer, the convergence zone is formed by the flows from the Atlantic cold tongue and the Saharan heat low, locating around 20°N (Nicholson, 2009, 2013). In NH winter, the anticyclonic wind from northern Africa converges with the southerly wind from Atlantic. The ITCZ over western Africa still stays in the continent (Nicholson, 2013). Therefore, the seasonal migration of the ITCZ in western Africa is within a narrower range of latitudes than in eastern Africa.

8: Line 276-277 Figure 6 shows significant seasonal variation for biomass burning CO. Surprisingly, the seasonal variation of biogenic isoprene is ignorable, which seems inconsistent with other study (e.g. Marais et al. 2014). Is it associated with the color scale? On the other hand, the normalized magnitudes of seasonal variability (Figure 7) are comparable between CO and isoprene. Is it due to the usage of standard deviation in the calculation? The approach for normalization is confusing.

Marais, E. A., Jacob, D. J., Guenther, A., Chance, K., Kurosu, T. P., Murphy, J. G., Reeves, C. E., and Pye, H. O. T.: Improved model of isoprene emissions in Africa using Ozone Monitoring Instrument (OMI) satellite observations of formaldehyde: implications for oxidants and particulate matter, *Atmos. Chem. Phys.*, 14, 7693-7703, <https://doi.org/10.5194/acp-14-7693-2014>, 2014.

Thanks for the points. Yes, the narrow seasonal variation of biogenic isoprene shown in the old Fig. 6 indeed is due to the use of the color scale. We have edited the color scale in the figure (now Fig. 8) so that the seasonal variation of biogenic isoprene in Africa is better presented. Fig. 9 (old Fig. 7) shows the seasonal variability of isoprene and CO. The biogenic emission peaks in spring and autumn. The magnitude of biogenic isoprene is comparable to the results in Marais et al. (2014).

Normalization is not taken in this revision to avoid confusing.

9: Line 315-362 The discussion in this section is superficial. The authors discuss the contributions from various sources without detailed calculations. For example, the authors indicated: 1) “In boreal spring, a region with high ozone concentrations (>40 ppbv) appears in higher altitudes and ... mainly due to the highest biogenic emissions

in the NHAF” 2) “In boreal autumn, the locations of the ITCZ and the Hadley cell are similar to these in boreal spring. Ozone in the African middle troposphere ... attributed to stronger lightning NO_x emission” However, there is no evidence to demonstrate that the contributions from biogenic and lightning activities are evaluated carefully. The discussion is simply based on the spatial distribution of Figure 6. The biogenic and lightning activities are highly similar between spring and fall, and it is hard to explain why the spring-time O₃ is biogenic dominant, whereas autumn-time O₃ is lightning dominant.

Thanks for the comments. Aghedo et al. (2007) has suggested that the biogenic and lightning emissions are the two important sources influencing African middle and upper tropospheric ozone and affecting global tropospheric ozone burden. To further explore the differences between the situations in NH spring and in NH autumn, we have conducted 3 sensitivity experiments by switching off the biogenic, lightning, and biomass burning emissions, respectively. The separate contribution of the three sources to tropospheric ozone over Africa is shown in the supplementary file (Fig. S7). In HN spring and autumn, the influence of ozone from SHAF on Asia is small and similar (Fig. 7) so we can mainly focus on ozone in NHAF. It appears that in NH spring, elevated ozone abundances from biogenic emissions are higher than that from lightning NO_x emissions while in NH autumn, elevated ozone abundances from biogenic emissions are lower than that from lightning NO_x emissions (Fig. S7, and also see Aghedo et al. (2007)). We have revised our paper accordingly. We also have made the discussion in more depth in section 3.3.4.

10: Section 4.2 It seems that Figure 8 and Figure 9 are already sufficient for the discussion. I suggest to remove Figure 10 to make the paper more concise.

Thanks for the points. Fig. 10 (in the last version) has been removed.

Response to Comments by Anonymous Referee #2

This is a relatively straightforward analysis of the interplay of meteorological processes and atmospheric chemistry in venting out ozone and ozone precursors from Africa and reaching Africa. The manuscript is well written, the figures appropriate.

As the authors state- there is relatively little literature discussing Africa-to-Asia transport, so this is a welcome addition, despite it doesn't make use of the recommendation in the HTAP2 exercise to harmonize region definitions to allow comparability of results.

We thank the reviewer for the encouragement and for the valuable and thoughtful comments. In Fig. 1, we show the regional definitions in this study and in HTAP2, so the reader can have an idea for the similarity and difference between the two definitions.

A minor remark is that I don't see terribly much added value of the trajectory analysis in figure 12.

The trajectory analysis is improved in this revision as follows. (1) Trajectories in two more seasons, spring and autumn, are added for comparison between the four seasons instead of just between two seasons in the last version, (2) trajectories from four more stations in Africa are added for a wider coverage and representation, (3) the mean transport paths for the trajectories that arrive Asia are illustrated with lapse times indicated, and (4) more discussions are added in this revision to supplement the discussion on the mechanisms that control the transport of African ozone to Asia throughout section 3.3, in section 4.2, and in the conclusions (section 5).

Although some attempt has been made to demonstrate the model's ability to model ozone over Africa, I think this could be done more convincingly- there is meanwhile a host of other observations (surface, aircraft, satellite tropospheric ozone columns) that could be explored.

Thanks for the point. In this revision, we add more validations between the

ozonesonde observations and GEOS-Chem simulations from perspectives of variceal profiles and the seasonal and interannual variability of tropospheric ozone over Africa in the surface layer, lower, middle, and upper troposphere. The comparisons at three more ozonesonde stations in India are added. Furthermore, the ozone data from the Tropospheric Emission Spectrometer (TES) satellite instrument are used to evaluate the GEOS-Chem simulation in the middle troposphere (464 hPa) globally in the supplementary file (Fig. S6). The detailed comparisons are shown in Figs. 2-4 and Tables 1-2 and are discussed in section 2.2.

Are signals from African ozone visible in soundings over India?

The transport of air mass from Africa in summer is reflected in the ozonesonde data at Poona and Thiruvananthapuram in western India (in an added figure, Fig. 4). The impact of the Somali jet on the ozone in western India is obvious as low ozone concentrations appear in the lower troposphere in NH summer.

The organization and discussion of methods could be somewhat more systematic.

Thanks for the suggestions. The methods are reorganized and the presentation is polished in section 2.

I suggest that the authors explore somewhat further these aspects, and recommend the manuscript to be accepted after taking these major and minor comments below into account.

Thanks. We have followed these suggestions.

Minor comments.

1. 11-30 the abstract could be somewhat more explicit in describing the regions and attribution methodology.

Thanks. The abstract is rewritten to explicitly state the regional definitions and attribution methods.

l. 16 Replace boreal by NH winter. Or find better way of describing which months are discussed. Are the > and < really meant to express minima and maxima?

Thanks. We have replaced boreal winter with northern hemisphere (NH) winter in this revision. We have removed the > and <, and used certain numbers to express minima and maxima.

l. 30 I miss some statement on the relevance of this analysis. How much of the Asian ozone was produced in Africa or from African precursor emissions- where is it most important (not only vertical but also geographically).

Vertically, the influence of African ozone on Asia is mainly in the middle and upper troposphere. Geographically, the imported African ozone mainly distributes over latitudes south to 40°N in Asia. We have added more detail about this in the abstract.

l. 35 give reference time to which this RF estimate pertains.

Thanks. The reference time is given: "It also acts as a greenhouse gas, whose global mean radiative forcing is about $0.4 \pm 0.2 \text{ W/m}^2$ for the period 1750-2011 (Myhre et al., 2013)".

l. 46 add: as well as a range of papers in the HTAP2 (Galmarini 2016) special issue.

Thanks. Galmarini et al. (2017) and several other papers in the HTAP2 special issue are now added in the citations.

l. 53 The issue is also very connected to legislative issues related to the control of ozone and ozone exceedance in the western states of the USA, e.g. as discussed in Huang et al. (2017; already cited).

Thanks. This point is now included in Introduction.

l. 54 One reference on LRT transport between South Asia and East Chakraborty et al. Science of the Total Environment, 523, 2015

Thanks for this recommendation. The reference is helpful to the study and it is added

in the reference.

l. 73 ... makes a contribution ... how is contribution defined? Zero out of emissions?

This is important because later you present a different method.

We have clarified this term in Introduction. In this study, we used the tagged ozone simulation to track ozone from source regions to a receptor region. We did not use the perturbation simulations that turn the emissions off to see the contribution of source regions to a receptor region.

The contribution of the source regions to the receptor region can be presented as absolute and fractional contributions. The former refers to the concentrations of the imported ozone in a unit of ppbv, while the latter is the ratio of the imported ozone to the total ozone in a grid, a layer, or a region. We have also described the term in Introduction and rephrased this sentence to make it clear.

l. 117 which resolution is used for GEOS-CHEM; what was the underlying resolution of the assimilation product. Importantly for this paper, how is convection parameterized, is there any evaluation over Africa of these process. Interhemispheric mixing and similar: refer to any relevant application of the model that demonstrates it is fit-for-purpose for this study. I realize that these are discussed later, but I would have expected these descriptions here.

Thanks for these comments. The detailed descriptions of GEOS-Chem have been moved to an earlier part in section 2.1. In this study, the simulations are driven by GEOS-4 meteorology at a 4° latitude by 5° longitude horizontal resolution, degraded from their native resolution of 1° latitude × 1.25° longitude. There are 30 vertical layers including 17 levels in the troposphere (see the 2nd paragraph in section 2.1). GEOS-4 uses the schemes developed by Zhang and McFarlane (1995) for deep convection and by Hack (1994) for shallow convection. GEOS-4 meteorology is found to be characterized with stronger deep convection in tropics than GEOS-5 (Liu et al., 2010; Zhang et al., 2011). Liu et al. (2010) and Zhang et al. (2011) have shown good agreement of GEOS-Chem simulations driven by GEOS-4 with satellite observations

in the tropical troposphere. Choi et al. (2017) compared the simulations of the Global Modeling Initiative (GMI) chemistry and transport model (CTM) driven by three meteorological data sets (fvGCM for 1995, GEOS-4 for 2005, MERRA for 2005) with ozonesonde and TES observations. They found that ozone simulated by GEOS-4 has the highest correlation with the observations. These previous studies and the good validation results over Africa from this study provide us confidence on the model performance. We have provided more details on the model descriptions in this revision (see section 2.1).

1. 125- If I understand correctly the authors merge the EDGAR3.2 global inventory with regional ones. Which period? How do these inventories compare with e.g. the HTAP2 inventory for 2008/2010 in this special issue, or EDGAR4.2 products (for time series).

We conducted the full chemistry simulation in GEOS-Chem to generate ozone production and loss data in 2005. The merged emission data are from the global EDGAR 3.2 inventory in the base year 2000. The regional emission inventories include the INTEX-B Asia emissions inventory in 2005 with base year 2006, the NEI05 inventory in North America in the base year 2005, the EMEP inventory in Europe in the base year 2005, the BRAVO inventory in Mexico in 2005 with base year 1999, and the CAC inventory in Canada in the base year 2005. This part has been described in more details in section 2.1.

We compared the anthropogenic emissions of CO and NO_x from the GEOS-Chem for 2000 inventories with those in the HTAP2 inventories for 2008 (http://edgar.jrc.ec.europa.eu/htap_v2/) and showed the comparison in the supplementary file (Figs. S3 and S4). Compared to the HTAP2 inventory for 2008, the CO and NO_x emissions in GEOS-Chem are lower in Africa throughout the year. The annual anthropogenic emissions of CO in Africa in GEOS-Chem and from the HTAP2 inventory are about 12.2 Tg yr⁻¹ and 62.5 Tg yr⁻¹, respectively. The anthropogenic emissions for NO_x in Africa in GEOS-Chem and HTAP are about 2.27 Tg yr⁻¹ and 4.53 Tg yr⁻¹, respectively

The contribution of anthropogenic emissions to generation of African ozone is considered to be smaller than that of other emissions. Aghedo et al. (2007) estimated that anthropogenic emissions emitted in Africa account for approximately 11% (4.7Tg/42.8Tg) of the total African emissions that impact the global tropospheric ozone burden. In this study, the annual biomass emissions of CO in Africa in GEOS-Chem are 182.8 Tg yr⁻¹, which is much larger than anthropogenic emissions of CO (4.7Tg yr⁻¹). Nevertheless, we should consider the impact of this issue and we have stated in this revision that “Although the anthropogenic emissions contribute less significantly to the ozone generation in Africa than biogenic, biomass burning, and lightning emissions (Aghedo et al., 2007), the differences between these emission inventories imply that African ozone simulated by GEOS-Chem is with some uncertainties.” (Line 187-190). .

1. 135 What is the global lightning source strength and specific for Africa. How does this compare to other studies.

Lightning NO_x emission used in the study is shown by annual mean and in each season in the supplementary file (Fig. S1). The annual global lightning NO_x source amount is 5.97 Tg N yr⁻¹, comparable to 6±2 Tg N yr⁻¹ in Martin et al. (2007) and 6.3 Tg N yr⁻¹ in Miyazaki et al. (2014). Miyazaki et al. (2014) estimated the annual global lightning NO_x emission by assimilating observations of NO₂, HNO₃, and CO measured by OMI, MLS, TES, and MOPITT into the global chemical transport model CHASER. The annual lightning emission is 1.72 Tg N month⁻¹ in Africa, 0.80 Tg N month⁻¹ in NHAf, and 0.79 Tg N month⁻¹ in SHAF, shown in the supplementary file. We have added the information in section 2.1 in the 3rd paragraph.

1. 137 briefly describe what is the ‘standard’ tagged ozone method. Pro’s and con’s-limitations. Comes now later

The tagged ozone method tracks ozone that is generated in different regions. The method was first proposed by Wang et al. (1998) and then further developed and used by a number of studies (Fiore et al., 2002; Sudo and Akimoto, 2007; Zhang et al., 2008;

Liu et al., 2011; Sekiya and Sudo, 2012, 2014; Zhu et al., 2017b). This is one of the standard modes in GEOS-Chem. It is done by the following two steps. First, the daily production rates and loss frequencies of odd oxygen ($O_x = O_3 + NO_2 + 2NO_3 + 3N_2O_5 + HNO_3 + HNO_4 + PAN + PMN + PPN$) were generated and archived from a full chemistry simulation before the tagged ozone simulation. Since ozone accounts for most of O_x , ozone instead of O_x is used for clarity. Second, GEOS-Chem is run again in the tagged ozone mode using the archived ozone production rate and loss frequency, with separate tracers for the ozone produced from each of the specific source regions. Therefore, the tagged ozone tracer method can assess the contributions of African ozone to Asia. The advantages of and issues with the tagged ozone simulation are discussed in section 2.1 (see the last paragraph in section 2.1) with an additional figure in the supplementary file (Fig. S5).

1. 138 I expected this description earlier.

Thanks. The description has been moved into an earlier part of the section. Please see the 2nd paragraph in section 2.1.

1. 140- 143: better include with the GEOSCHEM description.

Thanks. This part has been included with the GEOS-Chem description. Please see the 2nd paragraph in section 2.1.

1. 150- what is the reason for not simply taking the ‘african mask’ - instead two blocks.

I suggest adding a simple figure, showing these masks on top of a map (perhaps along with the HTAP2 definition of Africa).

Thanks for the suggestion. Fig. 1 is added to show the definitions of the source and receptor regions in this study. The definition of Africa in HTAP2 is also presented to show the similarity and difference between the two definitions. The reason for using the blocks to define regions is because this is the default way that GEOS-Chem uses for the tagged ozone simulation.

1. 155 I think most papers that I know keep (anthropogenic) emissions constant- but that is not necessarily the same as keeping the production terms constant. What could be the impact?

Thanks for this comment. Meteorology affects both chemistry and transport, a physical process. If keeping ozone production term constant, the meteorology influence on chemistry is ignored. If keeping emissions constant, the impacts of meteorology on both chemistry and transport are considered. We have pointed this out in this revision (section 2.1, the last 2nd paragraph).

1. 175- what about sfc observations, tropospheric residual from satellite. The comparison is fairly superficial

Thanks. In this revision, we have included more comparisons between the GEOS-Chem simulations and ozonesonde observations by adding 2 figures and two tables. The seasonal and interannual variation GEOS-Chem simulations have been further compared with ozonesonde data in the surface layer, lower, middle, and upper troposphere at the African sites. Three ozonesonde stations at India are added for the comparison. Figs. 2 and 3 and Tables 1 and 2 are added in section 2.2. The correlation coefficient (r), bias in percentage, and root-mean-square error (RMSE) between the simulations and the ozonesonde data are presented. The comparison in global distribution with the TES satellite ozone data are shown in the supplementary file (Fig. S6).

1. 201 Imported ozone=>try to describe more exactly what it is. Region-average abundance of imported ozone (imported ozone could be also the flux through the western border, for instance).

Thanks for the point. We define ozone that is generated over Africa under the tropopause as African ozone. Following Holloway et al. (2008), “Imported ozone” is used to refer ozone that is distributed over the receptor region. In the paper, when we discuss African ozone over Asia, we use “imported African ozone” to differentiate it from the overall ozone concentrations in Asia. We have clarified this term in

Introduction (the last paragraph in section 1).

p. 295 /figure 6: I guess if the units are molec/cm²/s this pertains to the integrated amount over a model layer; otherwise it should rather be per cm³?

Thanks for the point. Yes, in the last version, the unit pertains to the integrated NO_x amount over a model layer. We have converted the unit into NO_x emissions per cubic meter per second. Therefore, the lightning NO_x emissions are expressed as molec/m³/s in this revision (see Figs. 8 and 9).

带格式的: 左

Characteristics of intercontinental transport of tropospheric ozone from Africa to Asia

带格式的: 字体: 12 磅

Han Han¹, Jane Liu^{1,2}, Huiling Yuan¹, [Bingliang Zhuang¹](#), Ye Zhu^{1,3}, Yue Wu¹, Yuhan Yan⁴, Aijun Ding¹

带格式的: 字体: 12 磅

带格式的: 字体: 12 磅, 非上标/下标

¹School of Atmospheric Sciences, Nanjing University, Nanjing, China

²Department of Geography and Planning, University of Toronto, Toronto, Canada

³Shanghai Public Meteorological Service Centre, Shanghai, China

带格式的: 字体: 12 磅

⁴Chinese Academy of Science, Institute of Atmospheric Physics, Beijing, China

Correspondence to: Jane Liu (janejj.liu@utoronto.ca)(janejj.liu@utoronto.ca)

带格式的: 左

带格式的: 字体颜色: 文字 1

Abstract. ~~Based on 20-year simulations using~~

~~In this study, we characterize the transport of ozone from Africa to Asia through the analysis of the simulations of a global chemical transport model, GEOS-Chem, from 1987 to 2006. The receptor region Asia is defined within 5°N-60°N and a trajectory model, HYSPLIT, the transport of ozone produced 60°E-145°E, while the source region Africa is within 35°S-15°N and 20°W-55°E and within 15°N-35°N, 20°W-30°E. The ozone generated in the African troposphere to Asia is investigated. The study shows from both natural and anthropogenic sources is tracked through tagged ozone simulation. Combining with analysis of trajectory simulations using the Hybrid Single-Particle Lagrangian Integrated Trajectory (HYSPLIT) model, we find that the influence of African ozone on Asia varies largely upper branch of the Hadley cell connects with the subtropical westerlies in time and space. In the northern hemisphere (NH) to form a primary transport pathway from Africa to Asia in the middle and upper troposphere; throughout the inflow year. The Somali jet that runs from eastern Africa near the equator to the Indian subcontinent in the lower troposphere is the second pathway that appears only in NH summer.~~

~~The influence of African ozone to mainly appears over Asia peaks around 25°N, being the south of 40°N. The influence shows strong seasonality, varying with latitude.~~

longitude, and altitude. In the Asian upper troposphere, imported African ozone is largest in boreal winter and early spring (>10 ppbv from March to May around 30°N (12-16 ppbv) and the lowest in boreal summer (<6 ppbv during July-October around 10°N (~ 2 ppbv)). In the Asian middle and lower troposphere, imported African ozone ranges 2-6 ppbv over Asia, being highest in boreal peaks in NH winter between 20 - 25°N . Over 5 - 40°N , the mean fractional contribution of imported African ozone to the overall ozone concentrations in Asia is largest during NH winter (~ 4 ppbv) in the middle troposphere ($\sim 18\%$) and lowest in boreal fall (~ 2 ppbv). The NH summer throughout the tropospheric column ($\sim 6\%$).

This seasonality of the transport mainly results from the collective effects of the ozone precursor emissions in Africa, and meteorology and chemistry in Africa and Asia and along the transport pathways. The seasonal swing of the Hadley circulation and subtropical westerlies along the primary transport pathway plays a dominant role in modulating the seasonality. There is more imported African ozone in the Asian upper troposphere in NH spring than in winter. This is likely due to more ozone in the NH African upper troposphere from biogenic and lightning NO_x emissions in NH spring. The influence of African ozone on Asia appears larger in NH spring than in autumn. This can be attributed to higher altitudes of the elevated ozone in Africa and stronger subtropical westerlies in NH spring. In NH summer, African ozone hardly reaches Asia because of the blockings of Saharan High, Arabian High, and Tibetan High on the transport pathway in the middle and upper troposphere, in addition to the northward swing of the subtropical westerlies. The seasonal swings of the Intertropical Convergence Zone (ITCZ) in Africa and subtropical westerlies along the transport pathways. These meteorological conditions combined, coinciding with the seasonality geographic variations of ozone precursor the emissions from various sources in Africa, can further modulate the influence of African ozone on Asia. seasonality of the transport of African ozone, owing to the functions of the ITCZ in enhancing lightning NO_x generation and uplifting ozone and ozone precursors to upper layers. The strength of the ITCZ in Africa is also found to be positively correlated with the interannual variation of the transport of African ozone to Asia in NH winter.

带格式的
带格式的
带格式的
带格式的
带格式的
带格式的
带格式的

Ozone from ~~the northern hemispheric~~NH Africa ~~accounts for~~makes up over 7080% of the total imported African ozone over Asia in most altitudes and seasons. The interhemispheric transport of ozone from the southern hemispheric Africa is ~~observed~~ most ~~evidently~~evident in ~~boreal~~NH winter over the Asian upper troposphere and in ~~boreal~~NH summer over the Asian lower troposphere. The former case is facilitated ~~by~~associated with the ~~convective divergence~~primary transport pathway in the upper troposphere over the ITCZ in AfricaNH winter, while the latter ~~is driven by the Somali jet~~. ~~In boreal winter, the intensity of the ITCZ in Africa is positively correlated with the interannual variation of imported African ozone over Asia, because a stronger case is with the second transport pathway. The intensities of the ITCZ can uplift more surface ozone and ozone precursors and enhance lightning NO_x generation, resulting in more African ozone transported to Asia~~ in Africa and the Somali jet can respectively explain ~30% of the interannual variations in the transport of ozone from the southern hemispheric Africa to Asia in the two cases.

带格式的: 左, 缩进: 首行缩进: 0.42 厘米

带格式的

带格式的

带格式的

带格式的: 左, 行距: 1.5 倍行距, 无孤行控制

带格式的: 左

1 Introduction

Tropospheric ozone is a major air pollutant, harmful to human health (Anenberg et al., 2010), agricultural crops, and natural ecosystems (Hollaway et al., 2012; Lefohn et al., 2017). It also acts as a greenhouse gas, whose global mean radiative forcing is about $0.4 \pm 0.2 \text{ W/m}^2$ for the period 1750-2011 (Myhre et al., 2013). The dominant source of tropospheric ozone is from the photochemical reactions in which volatile organic compounds (VOCs) and carbon monoxide (CO) are oxidized in the presence of nitrogen oxides (NO_x) (Lelieveld and Dentener, 2000). Transport of ozone from the stratosphere downward is another ~~important~~ source of tropospheric ozone (Neu et al., 2014; Akritidis et al., 2016). Due to its ~~relatively long~~ lifetime (of days to weeks in the free troposphere),₂ ozone can be transported over long distances across continents, as seen~~shown~~ in a wealth of observation evidence (Huntrieser et al., 2005; Lewis et al., 2007; ~~Rastigejev et al., 2010~~; Verstraeten et al., 2015). Consequently, tropospheric ozone in a region is greatly influenced by ozone transport from upwind regions (Doherty et al., 2013; ~~Derwent et al., 2015, 2017~~). Therefore, intercontinental transport

of ozone has been a significant issue to scientists, public, and policymakers concerned with air quality and climate change (HTAP, 2010; Cooper et al., 2015; Doherty, 2015; [Huang et al., 2017](#)).

There have been numerous studies on the ~~three~~ major source-receptor relationships in the ~~Northern Hemisphere~~[northern hemisphere \(NH\)](#) for ozone transport among Asia, North America, and Europe, which are trans-Pacific (Jaffe et al., 2003; Zhao et al., 2003; Cooper et al., 2010; [Nopmongcol et al., 2017](#)), trans-Atlantic (Wild et al., 1996; Cooper et al., 2002; Guerova et al., 2006; [Derwent et al., 2015](#); [Karamchandani et al., 2017](#); [Knowland et al., 2017](#)), and trans-Eurasian (Wild et al., 2004; Fiore et al., 2009; Li et al., ~~2014~~[2014b](#)) [transport](#). The trans-Pacific transport from Asia to North America has been studied most because of ~~high pollutant emissions in Asia and their~~[the efficient eastward export of high pollutants in Asia and the close connection to legislative issues related to the control of ozone in USA](#) (Cooper et al., 2010, 2011, 2015; Verstraeten et al., 2015; Huang et al., 2017; Lin et al., ~~2017~~[2017](#)). [Developing a better understanding of the intercontinental transport of ozone across the NH is one of the main objectives for the Task Force on Hemispheric Transport of Air Pollution \(TF HTAP\) \(Galmarini et al., 2017, <http://www.htap.org>\).](#)

Transport of ozone to Asia from various source regions in the world has [been less documented but](#) received ~~some~~[increasing](#) attention ~~recently~~[since the 2000s](#) (Holloway et al., 2008; Nagashima et al., 2010; Wang et al., 2011; Li et al., ~~2014~~[2014b](#); [Chakraborty et al., 2015](#); Zhu et al., 2016; Zhu et al., 2017b). ~~Imported ozone, its seasonal variation, and spatial~~[The distribution depend on of foreign ozone in Asia is modulated by](#) numerous processes, involving chemistry (~~Wild et al., and 2004; Li et al., 2014~~), and meteorology in [both Asia, and the various source regions, and as well as](#) along the transport pathways ([Wild et al., 2004; Li et al., 2014b](#)). Previous studies illustrated the important role that meteorology plays in these processes (Sudo and Akimoto, 2007; Sekiya and Sudo, 2012, 2014; Zhu et al., 2017b). ~~Governed~~[For example, governed](#) by the westerlies in the ~~Northern Hemisphere~~[NH](#), the influence of European and North American ozone [on Asia](#) is larger in higher latitudes than in lower altitudes ~~of Asia~~ (Wild et al., 2004; Holloway et al., 2008; Zhu et al., 2017b). The

seasonal switch in Asian monsoonal winds significantly affects the seasonal variation of ozone transported to Asia (Nagashima et al., 2010; Wang et al., 2011; Zhu et al., 2017b). The Asian monsoon anticyclone (South Asian High, SAH) ~~has remarkable effects on~~ can also modulate the movement of ozone in the upper ~~tropospheric ozone transport~~ troposphere over Eurasia (Vogel et al., 2014; Garny and Randel, 2016).

Africa covers areas from the ~~Northern Hemisphere~~ NH to the Southern Hemisphere; (SH), with around three quarters of the continent ~~are located~~ in the tropics. Comparing with other continents, Africa has the most frequent lightning (Albrecht et al., 2016) and the largest burned areas (Giglio et al., 2013). ~~Over~~ Approximately, 70% of tropospheric ozone produced ~~in Africa from natural and anthropogenic sources~~ over the African troposphere is exported out of Africa (Aghedo et al., 2007), making African ozone an obvious influence on the global tropospheric ozone budget (Piketh and Walton, 2004; Thompson, 2004; Williams et al., 2009; Bouarar et al., 2011; Zare et al., 2014). ~~There have been a few studies~~ Nevertheless, there is relatively little literature on the transport of African ozone to ~~some locations in~~ Asia (Liu et al., 2002; Sudo and Akimoto, 2007; Lal et al., 2014). By tagging ozone from Africa in a global chemistry transport model, Liu et al. (2002) ~~found~~ reported that African ~~outflow makes a contribution of~~ ozone contributed about 10-20 ppbv to the overall ozone concentrations in the middle and upper troposphere ~~over~~ at Hong Kong, ~~southeast of~~ China, during the November-April period. Sudo and Akimoto (2007) showed that there is a significant interhemispheric ozone transport from South America to Japan in the upper troposphere in conjunction with ozone export from northern Africa. Lal et al. (2014) reported that the ozone distribution over western India in the lower troposphere during the summer monsoon ~~seasons~~ season is affected by long-range transport from the east coast of Africa. ~~Nevertheless, questions still remain~~ These previous studies mostly focused on ~~how and how much~~ the transport of African ozone ~~is transported to~~ some locations in Asia. It is unclear to which degree that African ozone influences Asia regionally, how the transport pathways vary with season, and ~~their seasonality, as well as~~ what underlying mechanisms ~~for~~ modulate the transport.

The Intertropical Convergence Zone (ITCZ), defined as the convergence of the trade

带格式的: 字体: 12 磅

winds, is one of the most prominent meteorological phenomena in the tropics (Waliser and Gautier, 1993; Žagar et al., 2011; Suzuki, 2011). ITCZ is a heat engine driving the ascending branch of the Hadley circulation (Nicholson, 2009; Suzuki, 2011). ITCZ and its seasonality can significantly impact the meteorological conditions over Africa (Nicholson, 2009; Collier and Hughes, 2011; Suzuki, 2011). Characterized with deep and strong convection, the equatorial region between the ITCZ branches is a region with effective interhemispheric mixing (Avery et al., 2001). ~~Meanwhile, the ITCZ can be a barrier to interhemispheric exchange in the lower troposphere (Raper et al., 2001).~~ The convective divergence in the upper troposphere over the ITCZ was proposed to be one of the primary mechanisms for the interhemispheric transport (Hartley and Black, 1995; Avery et al., 2001). Meanwhile, the ITCZ can be a barrier to interhemispheric exchange in the lower troposphere (Raper et al., 2001). ~~Based on aircraft and satellite observations, an anti-correlation was found between ozone abundances and convective outflow over central American ITCZ region by Avery et al. (2010).~~ Together with the Southeast Asian monsoon, the movement of the ITCZ can modulate pollution transport to Southeast Asia (Pochanart et al., 2003, 2004). In addition, the ITCZ over western Africa is found to play a significant role in controlling the transport of Saharan mineral dust to northern South America, modifying ~~its~~ air quality and climate ~~there~~ (Piketh and Walton, 2004; Doherty et al., 2012, 2014; Rodríguez et al., 2015). However, the ~~influence~~influence of the ITCZ on ozone transport from Africa to Asia ~~have~~has not been well understood.

带格式的：英语(加拿大)

In this ~~study paper, we present~~ a comprehensive ~~investigation is made~~study on the transport of African ozone to Asia through ~~integrated numerical~~ analysis of tagged ~~tracer and ozone simulations, as well as~~ trajectory simulations. In this paper, the term “African ozone ~~here~~” refers to ozone that is generated in the African troposphere below the tropopause from ~~at~~both natural and anthropogenic sources, as Sudo and Akimoto (2007) suggested that ~~investigation~~investigating the contributions of both ~~sources to~~ ozone production ~~from both sources~~ is necessary. The term “imported African ozone” or “imported ozone” refers to the African ozone that has been transported to and distributed over Asia, and it refers to African ozone concentrations

- 带格式的：字体颜色：自动设置
- 带格式的：字体颜色：黑色
- 带格式的：字体颜色：黑色
- 带格式的：字体颜色：黑色
- 带格式的：字体颜色：黑色
- 带格式的

in the model grids in Asia. The source region Africa and the receptor region Asia are shown in Fig. 1. The contribution of the source regions to the receptor region is presented as absolute or fractional contribution. The former refers to the imported African ozone concentrations in ppbv, while the latter is the ratio of the imported ozone concentrations to the overall ozone concentrations in the model grids in Asia.

Our specific objectives are (1) to characterize the seasonal ~~variation~~variations of ozone transport from Africa to Asia, (2) to investigate the underlying mechanisms responsible for such seasonal ~~variation~~variations, and (3) to ~~explore a possible connection between~~find meteorological influences, including the ITCZ ~~and, on~~ the interannual variation of ~~imported~~the transport of African ozone ~~over to~~ Asia, including the interhemispheric transport from the SH. Our analysis is based on the simulations from a 3-dimensional global chemical transport model, GEOS-Chem (Bey et al., 2001a), for 20 years from 1987 to 2006 ~~and simulations from a,~~ supplemented by the analysis of trajectory ~~climatology for the same periods~~simulations from the Hybrid Single-Particle Lagrangian Integrated Trajectory model (HYSPLIT) (Draxler and Hess, 1998; Stein et al., 2015). In section 2, ~~we describe the two models~~GEOS-Chem and the tagged ozone stimulation method are described, followed by the comparison of GEOS-Chem simulations with ozonesonde and satellite data. The HYSPLIT model and the meteorological data used in this study. The validation of GEOS-Chem simulations is are also presented in described. Section 3 is the core section 2. ~~We address the first objective in section 3 and the second and third in section 4. Section 5 offers an overview of that discusses the processes involved~~seasonality of imported African ozone over Asia and possible underlying mechanisms. In section 4, meteorological influences on the interannual variation in the transport of African ozone to Asia-, including the interhemispheric transport, are explored. Finally, ~~the~~ conclusions are drawn with discussion in section ~~6~~5.

带格式的：英语(加拿大)

2 MethodologyModels and data

2.1 The description of the GEOS-Chem model ~~and its validation~~

A global 3-dimensional chemistry transport model, GEOS-Chem (version v9-02) (Bey

et al., 2001a, <http://geos-chem.org>), is employed to simulate the global ozone distributions and the source-receptor ~~relationships~~relationship between Africa and Asia. GEOS-Chem includes a detailed ~~simulation~~description of tropospheric O₃-NO_x-hydrocarbon-aerosol. It is driven by assimilated meteorological data from the GEOS at NASA Global Modeling and Assimilation Office (GMAO). ~~The model has been used extensively in studying pollution transport (Bey et al., 2001b; Koumoutsaris et al., 2008; Zhang et al., 2008; Liu et al., 2011; Wang et al., 2011; Ridder et al., 2012; Long et al., 2015; Jiang et al., 2016; Huang et al., 2017; Ikeda et al., 2017; Zhu et al., 2017a; Zhu et al., 2017b).~~

In this study, the simulations are driven by GEOS-4 meteorology at a 4° latitude by 5° longitude horizontal resolution, degraded from their native resolution of 1° latitude by 1.25° longitude. There are 30 vertical layers including 17 levels in the troposphere. Transport and chemical timesteps are 10 minutes and 20 minutes, respectively, as suggested by Philip et al. (2016). In this version of GEOS-Chem, the GEOS-4 uses the deep convection scheme of Zhang and McFarlane (1995) and the shallow convection scheme of Hack (1994). By comparing the GEOS-Chem simulations driven by GEOS-4 and GEOS-5 with satellite observations in the tropical troposphere, Liu et al. (2010) and Zhang et al. (2011) have found GEOS-4 has stronger deep convection in the tropics than GEOS-5. In general, GEOS-Chem driven by GEOS-4 can simulate tropospheric ozone concentrations that are in good agreement with ozonesonde observations (Liu et al., 2010; Zhang et al., 2011; Choi et al., 2017; Zhu et al., 2017b).

GEOS-Chem has various modes that serve different simulation goals. In the full chemistry simulation, the emission inputs for a specific year are scaled from each inventory's base year. The global anthropogenic emission inventories are from EDGAR 3.2 for NO_x, CO, SO_x (Olivier and Berdowski, 2001) and RETRO for VOC emissions (Pulles et al., 2007); in 2000, merged with the following regional inventories: the INTEX-B Asia emissions inventory in 2006 (Zhang et al., 2009), the US Environmental Protection Agency National Emission Inventory in 2005 (NEI05) for North America, the Cooperative Programme for Monitoring and Evaluation of the Long-range Transmission of Air Pollutants in Europe (EMEP) inventory for Europe

带格式的：左

带格式的：字体颜色：自动设置

(Vestreng and Klein, 2002), in 2005, Big Bend Regional Aerosol and Visibility Observational (BRAVO) Study Emissions Inventory for 1999 in Mexico (Kuhns et al., 2003), and the Criteria Air Contaminants (CAC) inventory for Canada. The emission inventories for China and SE Asia are based on Streets et al. (2003, 2006), in 2005. Biofuel emission inventory is emissions are from Yevich and Logan (2003). Biomass burning and Biogenic biogenic emissions are from the GFED3 inventory (van der Werf et al., 2010) and MEGAN 2.1 (Guenther et al., 2012) respectively. Lightning NO_x emissions are calculated with the scheme of Allen et al. (2010) and the vertical distribution suggested by Ott et al. (2010). The annual global lightning NO_x emissions is 5.97 Tg N yr⁻¹, comparable to 6±2 Tg N yr⁻¹ in Martin et al. (2007) and 6.3 Tg N yr⁻¹ in Miyazaki et al. (2014). The annual total lightning NO_x emission in Africa is 1.6 Tg N yr⁻¹, 0.80 Tg N yr⁻¹ in NHAF, and 0.79 Tg N yr⁻¹ in SHAF (see supplementary Figs. S1 and S2). The anthropogenic CO and NO_x emissions from GEOS-Chem for 2000 are compared with those in the HTAP2 emission inventories for 2008 (http://edgar.jrc.ec.europa.eu/htap_v2/) (Figs. S3 and S4). The annual anthropogenic CO emissions in Africa are 12.2 Tg yr⁻¹ for 2000 in GEOS-Chem, lower than 62.5 Tg yr⁻¹ for 2008 from the HTAP2 inventories. The anthropogenic NO_x emissions in GEOS-Chem are 2.27 Tg yr⁻¹ for 2000, also lower than 4.53 Tg yr⁻¹ for 2008 from the HTAP2 inventories. Although the anthropogenic emissions contribute less significantly to the ozone generation in Africa than biogenic, biomass burning, and lightning emissions (Aghedo et al., 2007), the differences between these emission inventories imply that African ozone simulated by GEOS-Chem is with some uncertainties.

带格式的: 字体颜色: 自动设置

To investigate the influence of African ozone on Asia, we used the standard mode for tagged ozone simulation in GEOS-Chem (Wang et al., 1998; Fiore et al., 2002; Zhang et al., 2008). The simulation is driven by GEOS-4 meteorology, which uses the deep convection scheme of Zhang and McFarlane (1995) and the shallow convection scheme of Hack (1994). The simulation covers a period from January 1986 to December 2006 (using 1986 for model spin-up) at 4° latitude by 5° longitude horizontal resolution with 30 vertical layers, 17 levels in the troposphere. Transport and

带格式的: 字体颜色: 自动设置, 英语(加拿大)

带格式的: 字体颜色: 自动设置

chemical timesteps used in the study are 10 minutes and 20 minutes, respectively, as suggested by Philip et al. track the transport of ozone generated in Africa, we use the tagged ozone mode in GEOS-Chem, in which odd oxygen is tagged ($O_x = O_3 + NO_2 + 2NO_3 + 3N_2O_5 + HNO_3 + HNO_4 + PAN + PMN + PPN$, Fiore et al., 2002; Zhang et al., 2008). Since ozone accounts for most of O_x , we refer to ozone instead of O_x for clarity. To prepare for the tagged ozone simulation, we first run GEOS-Chem in the full chemistry simulation before the tagged simulation (Zhang et al., 2008; Liu et al., 2011). The source mode to generate the daily ozone production rate and loss frequency. Then we run GEOS-Chem in the tagged ozone mode to differentiate ozone produced in different source regions, tagged as different tracers, by using the archived daily ozone production rates and loss frequencies. As shown in Fig. 1, the source region, Africa, is defined as the region of 35°S-15°N, 20°W-55°E and 15°N-35°N, 20°W-30°E. Therefore, ozone produced in Africa below the tropopause from all natural and anthropogenic sources is tagged as a tracer. We further divide Africa into northern hemispheric Africa (NHAF) and southern hemispheric Africa (SHAF), which is further separated by the equator and thus added two tropospheric layers, the lower troposphere (LT, from the surface to 700 hPa), the middle troposphere (MT, 700-300 hPa), and the upper troposphere (UT, 300 hPa-tropopause) so to add six more tracers. The receptor region, Asia, is defined as the region of 5°N-40°N, 60°E-145°E.

In the simulation, for a year, both seasonal variation of chemistry and meteorology are both considered. To study the meteorological influence on the interannual variation, in the transport of African ozone to Asia, the tagged ozone simulation is conducted for 20 years from January 1986 to December 2006 (using 1986 for model spin-up). As our purpose is focused on the impact of meteorological influence on transport, we allow the meteorology on the transport of African ozone to

带格式的: 左, 缩进: 首行缩进:
2 字符

Asia. Therefore, the meteorology was set to vary from year to year, while a fixed but fix the chemistry was used for the 20-year simulation constantly, i.e., with using the archived daily ozone production and loss data in one year, i.e. 2005, for the 20-year simulation. This treatment is similar to the treatments in previous studies that examined the influences of meteorology on pollution transport (Liu et al., 2011; Zhao et al., 2012, 2005; Sekiya and Sudo, 2014; Zhu et al., 2017b). Note that meteorology affects both transport (a physical process) and chemistry while this treatment only considers the former.

To quantify accurately the contribution of different sources to ozone abundances in a receptor region using a numerical model, a good agreement between the model. Numerical approaches to exploring the source-receptor relationships include (1) tagged tracer simulations, (2) trajectory simulations, (3) perturbation simulations, and (4) inverse simulations (Zhu et al., 2017b). Compared with the other approaches, the tagged trace simulation can track ozone effectively from different source regions and to separate the contributions of ozone from different source regions to a receptor region and quantify each region's contribution. One issue with the tagged ozone simulation is the nonlinearity of chemistry. This nonlinearity can cause large differences between the full chemistry and the tagged ozone simulations. To test the scale of the nonlinearity in the simulations, ozone concentrations between the full chemistry and the tagged ozone simulations are compared at four ozonesonde sites in Africa and India (Fig. S5). The difference is found to generally within $\pm 5\%$, suggesting that this approach works in these regions without large bias.

2.2 The validation of GEOS-Chem simulations

GEOS-Chem has been used widely in studying pollution transport (Bey et al., 2001b; Koumoutsaris et al., 2008; Zhang et al., 2008; Liu et al., 2011; Wang et al., 2011; Ridder et al., 2012; Long et al., 2015; Jiang et al., 2016; Huang et al., 2017; Ikeda et al., 2017) and observations is required (Cooper et al., 2015; Derwent et al., 2016). Although the GEOS-Chem simulations have been extensively validated (Zhang et al., 2008; Liu et al., 2009; Wang et al., 2011; Kim et al., 2015; Zhu et al., 2017a; Zhu et al., 2017b), we

带格式的: 字体颜色: 自动设置

~~specifically validated the model in Africa). Tropospheric ozone simulated by GEOS-Chem has been extensively validated using ozonesonde and satellite data, such as in North America (Zhang et al., 2008; Zhu et al., 2017b), Europe (Kim et al., 2015), East Asia (Wang et al., 2011; Zhu et al., 2017a; Zhu et al., 2017b), and other regions (Liu et al., 2009). These validation practices have suggested reasonable agreements between the model simulations and ozone measurements. In this study, for an enhanced confidence on the model performance, ~~using the ozonesonde measurements~~ we compare the GEOS-Chem simulations with the ozonesonde data in Africa and India and with the satellite measurements from the Tropospheric Emission Spectrometer (TES) instrument. The ozonesonde data are acquired from the World Ozone and Ultraviolet Radiation Data Centre (WOUDC) (<http://www.woudc.org/home.php>). ~~We selected three~~ and the monthly TES product TL2O3LN is from the NASA Langley Atmospheric Science Data Center (https://eosweb.larc.nasa.gov/project/tes/tes_table).~~

带格式的: 英语(加拿大)

带格式的: 字体颜色: 文字 1

带格式的: 字体颜色: 文字 1

Three ozonesonde stations ~~at~~ in Africa are selected for their long record. The stations include Santa Cruz in North Africa (28.42°N, 16.26°W, 36 m), Nairobi in East Africa (1.27°S, 36.8°E, 1745 m), and Irene in South Africa (25.91°S, 28.21°E, 1524 m). ~~The~~ (Fig. 1). These ozonesonde observations data have been used in ~~studies on African~~ studying tropospheric ozone in Africa widely (Clain et al., 2009; Thompson et al., 2012, 2014). In Asia, comparisons between GEOS-Chem simulations and ozonesonde observations have been made by Liu et al. (2002) and Zhu et al. (2017b) at stations over the Pacific Rim, showing that GEOS-Chem can generally capture the vertical and seasonal variations of ozone concentrations in the region. We further compare the GEOS-Chem simulations at three Indian sites, including New Delhi in northern India (28.3°N, 77.1°E, 273 m), Poona in western India (18.53°N, 73.85°E, 559 m), and Thiruvananthapuram in southern India (8.48°N, 76.95°E, 60 m) (Fig. 1).

Fig. Fig. 12 shows the simulated and measured vertical ozone profiles by season, which are averaged from ~~1990~~1999 to 2003 ~~for~~at Santa ~~Cruz~~Cruz, from ~~1996~~2003 to 2006 ~~for~~at Nairobi, and from ~~1990~~1999 to ~~2006~~for2005 at Irene. ~~Fig. 3~~ by season. The simulations and the observations exhibit good agreements. ~~3~~ compares the time series.

of monthly ozone concentrations between the model simulations and ozonesonde measurements at different tropospheric layers at the sites. The corresponding bias, root-mean-square error (RMSE), and the correlation coefficient (r) between the two datasets are shown in Table 1 for the vertical profiles and in Table 2 for the time series, respectively.

For the ozone vertical profiles (Fig. 2 and Table 1), GEOS-Chem appears to reasonably capture the ozone vertical variation and its seasonality at the three sites. It appears that GEOS-Chem overestimates ozone in the upper troposphere at Santa Cruz in NH winter and spring and underestimates ozone in the upper troposphere at Nairobi in NH summer and autumn. The correlation coefficients between the two data are above 0.9 for most seasons at the three sites. The mean biases ranges from -9.3% (at Nairobi in October) to 23.2% (at Santa Cruz in January), while the RMSE ranges from 4.3 ppbv (at Nairobi in April) to 15.5 ppbv (at Santa Cruz in January). The bias and RMSE suggest that the model performs no better at a station or a season than the other stations or seasons.

For the time series of ozone at the upper, middle and lower troposphere, as well as the surface layer (Fig. 3 and Table 2), GEOS-Chem also performs reasonably well. The correlation coefficients between the two datasets in the tropospheric layers range within 0.57-0.79 at Santa Cruz, 0.76-0.90 at Nairobi, and 0.61-0.82 at Irene, all significant at a 95% significant level. The correlation coefficient is 0.60, 0.82, and 0.39 for the surface layer at Santa Cruz, Nairobi, and Irene, respectively. However, the model underestimates upper tropospheric ozone in Nairobi ~~in the four seasons and~~ (Table 2, Bias= -14.2%), somewhat ~~overestimates ozone~~ overestimate ozone in 500-300 hPa at Santa Cruz (Table 2, Bias= 4.5%) and near the surface ~~in at Irene-~~ (Table 2, Bias=60.3%).

The comparison between the GEOS-Chem and ozonesonde data at the three India sites is shown in a seasonal-altitude distribution in Fig. 4. The ozone concentrations are the means between 1994 and 2003. The time series of ozonesonde data at the sites are not shown because of inadequate records. The seasonal-altitude patterns of ozone at the three sites are well simulated, although the model overestimates the

带格式的：左

ozone near the surface and underestimates the ozone in the middle and upper troposphere at the three sites. The annual mean bias at New Delhi is 5.6%, -14.5%, and -18.9% in the lower (LT), middle (MT), and upper (UT) troposphere, respectively. At Poona, it is 2.1%, -5.6%, and -19.1% in the LT, MT, and UT, respectively, while the annual mean bias at Thiruvananthapuram is -4.4% in the LT, -13.3% in the MT, and -27.4% in the UT.

The global distribution of ozone from the GEOS-Chem simulations is compared with the TES observation in 2005 in the four seasons at 464 hPa (Fig. S6), a layer around which the TES satellite data have the least bias. The GEOS-Chem simulations are smoothed with the TES averaging kernels and *a priori*. The smoothed GEOS-Chem simulations resemble the GEOS-Chem simulations (not shown, see Jiang et al. 2016).

2.2 Generally, GEOS-Chem can capture the global variation of ozone in space and by season, such as the elevated ozone concentrations over the NH middle latitudes in NH spring and summer and the plumes of elevated ozone from biomass burning over southern Africa in NH autumn. The smoothed ozone concentrations are generally lower than the TES observation over Africa in all the seasons, with a maximum difference of 20 ppbv (or 20%). Note that TES ozone retrievals generally are higher than ozonesonde data, having a mean positive bias of 3-11 ppbv in the troposphere (Nassar et al., 2008).

Overall, GEOS-Chem can reasonably capture the seasonality of the ozone vertical profiles in the ozonesonde data over Africa. In Asia, GEOS-Chem tends to overestimate ozone in the lower troposphere and underestimate ozone in the upper troposphere at three Indian sites. The GEOS-Chem simulations also compare well with satellite TES data in space and by season.

2.3 The HYSPLIT trajectory model and meteorological data

We use HYSPLIT_4 (To supplement the analysis on the GEOS-Chem simulations, we use the Hybrid Single-Particle Lagrangian Integrated Trajectory model, version 4 (HYSPLIT-4) (Draxler and Hess, 1998; Stein et al., 2015) to simulate forward trajectories to show the outflows from Africa. With powerful computational

带格式的: 左

capabilities, and examine the transport pathways of African ozone to Asia. The HYSPLIT model is one of the most extensively used atmospheric transport and dispersion models (Fleming et al., 2012). Meteorological inputs to HYSPLIT are the NCEP reanalysis at a resolution of $2.5^{\circ} \times 2.5^{\circ}$ (<http://ready.arl.noaa.gov/archives.php>). Six-day forward trajectories were calculated from 1987 to 2006 four times a day (00, 06, 12 and 18 UTC) at seven African sites, including Cairo (31.1°E , 30°N , in North Africa), Ghat (10.2°E , 24.6°N), Khartoum (32.3°E , 15.4°N), Abuja (7.4°E , 9°N , in West Africa), and Juba (31.4°E , 4.5°N) in NHAF and Dar es Salaam (39.2°E , 6.8°S , in East Africa) and Johannesburg (28°E , 26.2°S , in South Africa), 5°S) and Luanda (13.1°E , 8.5°S) in SHAF (Fig. 1). The levels at 1.5 km, 5.5 km, and 11 km are selected to represent the trajectory starting altitude at the lower, middle, and the upper troposphere, respectively. The results were clustered for each month seven sites are chosen to represent two longitudinal and 3-4 latitudinal zones in Africa.

2.3 Meteorological data

The meteorological data include the NCEP/NCAR reanalysis I (Kalnay et al., 1996). The daily wind fields are used to describe the climatology of atmospheric circulation during the study period from 1987 to 2006. The product is available on a $2.5^{\circ} \times 2.5^{\circ}$ horizontal grid at 17 pressure levels from 1000 hPa to 10 hPa (<https://www.esrl.noaa.gov/psd/data/gridded/data.ncep.reanalysis.html>).

Additionally, the monthly Outgoing Longwave Radiation (OLR) data from NCAR at $2.5^{\circ} \times 2.5^{\circ}$ with temporal interpolation (Liebmann and Smith, 1996, https://www.esrl.noaa.gov/psd/data/gridded/data.interp_OLR.html) (https://www.esrl.noaa.gov/psd/data/gridded/data.interp_OLR.html) are used to indicate the intensity of the convection over ITCZ. The dataset has been widely used for tropical studies on deep convection and rainfall (Mounier and Janicot, 2004).

带格式的: 左, 缩进: 首行缩进: 0.42 厘米

带格式的: 左

带格式的: 字体颜色: 自动设置

带格式的: 左, 缩进: 首行缩进: 0.42 厘米

3 Seasonal ~~variation in imported~~ variations of the transport of African ozone over to Asia

3.1 Seasonal variations in African ozone over Asia

Because a substantial amount of ozone and ozone precursors are produced or emitted in Africa, tropospheric ozone in the other continents is largely influenced by ozone outflow from Africa (Williams Aghedo et al., 2009; Zare et al., 2014). Fig. 25 shows seasonal variations of imported African ozone in the Asian troposphere, varying with latitude and altitude. The values are the 20-year means (1987-2006) from the GEOS-Chem simulation. The largest African influences appear in the Asian middle and upper troposphere, i.e., 2-16 ppbv at 500 and 700 hPa. African ozone in the Asian lower troposphere is reduced to between 2 to 10 ppbv at 700 hPa throughout the year. Unlike imported European and North American ozone that influences Asia mostly over high altitudes (i.e., north of 30°N) (Wild et al., 2004; Holloway et al., 2008; Nagashima et al., 2010; (Zhu et al., 2017b), imported African ozone prevails over lower latitudes, generally south to between 5-40°N, considerably larger than European and North American ozone south of 30°N (Wild et al., 2004; Sudo and Akimoto, 2007; Zhu et al., 2017b). North of 50°N, African ozone influence is small, i.e., less than 4 ppbv and 2 ppbv, respectively, above and below the Asian middle troposphere. Seasonally, imported African ozone in the middle and upper troposphere peaks in March 25°N NH spring around 30°N (~16 ppbv, Figs. 2a and 2b Fig. 5a) and is at its minimum in July NH summer south of 25°N. Owing to the high radiative forcing efficiency, the change in ozone concentrations in the upper troposphere can impact climate more significantly than that in the lower troposphere (Lacis et al., 1990). Therefore, the influence of African ozone on the climate in southern Asia is likely larger than that of European and North American ozone (Aghedo et al., 2007; Sudo, In the middle troposphere (Fig. 5b), African ozone is at the maximum (~16 ppbv) in NH winter between 20°N and Akimoto, 2007): 25°N. In the lower troposphere (Fig. 2e5c), between 40-40°N, African ozone is high in boreal NH winter (~6-10 ppbv), while south of 45°N, African ozone peaks has another peak in boreal NH summer (~4 ppbv). Near the surface (Fig. 5d), African ozone

带格式的: 字体颜色: 自动设置

带格式的: 左

带格式的: 字体颜色: 自动设置

带格式的: 字体颜色: 自动设置

带格式的: 左

concentrations are low, i.e. below 4 ppbv.

—The strong seasonality of imported African ozone can also be shown vertically in Fig. 3a 6a, in which imported African ozone is averaged over Asia- south of 40°N.

The fractional contribution of imported African ozone to ozone in Asia is shown in

Fig. 3b6b. In the Asian upper troposphere, imported African ozone is the most largest

during February-March-May (⇒(over 10 ppbv) and the least during July-September

(←October (below 6 ppbv). Slightly different from the situation in the upper

troposphere, imported African ozone in the Asian-In the Asia middle troposphere is at

imported African ozone is at a minimum from July to September (~4 ppbv, 6% in the

fractional contribution) and a maximum (⇒(over 10 ppbv, 14% in the fractional

contribution) from December-January to April and at a minimum from June to

September (~4 ppbv, 6% March, about one month earlier than in the fractional

contribution)-upper troposphere. In the Asian lower troposphere, imported African

ozone is the largest in borealNH winter (~4 ppbv, 8% in the fractional contribution)

and lowest in boreal fallNH autumn (~2 ppbv, 5% in the fractional contribution).

Seasonal-altitude variations of

Furthermore, the total imported African ozone from NHAF and SHAF over Asia is

divided by tropospheric layer (UT, MT, and LT) and by hemisphere and the fractional

contributions of NHAF and SHAF ozone to the total imported African ozone are

contribution for each region is shown in Fig. 4. Ozone7. Over the Asian upper

troposphere, African ozone from the NHAF UT accounts for over 60-70% of the total

imported African ozone in the Asian tropospheric column (Fig. 7a), decreasing to ~20%

in the Asian MT (Fig. 7b) and to below 20% in the Asian LT (Fig. 7c). In the

meantime, the influence of African ozone from the NHAF MT becomes larger in the

Asian MT and LT (20-40%). So does the influence of African ozone from the NHAF

LT (20-40%). African ozone from SHAF contributes to the total imported ozone

throughout the year in the three tropospheric layers. The contribution is small, usually

below 20% of the total imported African ozone, except for in the upper troposphere in

borealNH winter over the Asian UT (Fig. 7a) and the lower troposphere in borealNH

summer. The summertime over the Asian LT (Fig. 7c). The two exceptions in

带格式的

带格式的

带格式的

~~interhemispheric transport of SHAF ozone to the Asian lower troposphere is also shown in a summer maximum of African ozone in Fig. 2c (-4 ppbv at 700 hPa, south of 15°N). This was also reported by Lal et al. (2014), who attributed it to ozone will be discussed in detail in section 4.2.~~

~~The seasonality of the transport from the Indian Ocean of African ozone to Asia results from the east coast collective impact of Africa.~~

带格式的: 英语(加拿大)

带格式的: 英语(加拿大)

带格式的: 英语(加拿大)

~~As African ozone mainly peaks in the Asian middle and upper troposphere, the horizontal distributions of African ozone at 400 hPa in January, April, July, and October overlaid with winds are shown in Fig. 5 to further illustrate its seasonality and transport pathways. Driven by the emissions of ozone precursors in the source region and the upper tropospheric easterly jet around meteorology and chemistry from the equator (Diedhiou et al., 1999), high African ozone appears across source region to the Atlantic, reaching the South America throughout the year receptor region. The westward transatlantic routes from northern Africa are built by the easterly waves (Jones et al., 2003; Mari et al., 2008; Ben-Ami et al., 2009). In boreal winter, near the northern and southern borders precursors of Africa, African ozone can be transported for a long distance along the subtropical westerly jets in the two hemispheres, reaching the western Pacific in the Northern Hemisphere and across Australia in the Southern Hemisphere, respectively. In boreal summer, the northern subtropical westerlies and tropical easterlies shift to their most northern positions; less African ozone can be transported to Asia than in the other seasons. However, around 40°N, the amount of African ozone being transported to Asia is similar to the other season (Fig. 2a).~~

带格式的: 英语(加拿大)

带格式的: 英语(加拿大)

带格式的: 英语(加拿大)

带格式的: 英语(加拿大)

带格式的: 英语(加拿大)

4 Possible mechanisms for the transport of African ozone to Asia

~~In this section, we analyze the transport pathways from Africa to Asia and associated underlying mechanisms so to cast some light on the spatial and seasonal variations in imported African ozone over Asia presented in section 3. Since Africa covers areas in both Northern and Southern Hemispheres with a large portion in the tropics, the atmospheric circulation over Africa experiences obvious seasonal changes induced by the seasonality of the ITCZ and the Hadley cell (Nicholson and Grist, 2003;~~

带格式的: 左, 缩进: 首行缩进: 0.42 厘米

~~Nicholson, 2008, 2009; Žagar et al., African ozone 2011; Suzuki, 2011).~~ African ozone precursors are mainly from biogenic sources, biomass burning, and lightning NO_x sources (Piketh and Walton, 2004; Thompson, 2004; Aghedo et al., 2007; Giglio et al., 2013; Monks et al., 2015). The seasonalities of emissions from biogeneticbiogenic sources, biomass burning, lightning, and anthropogenic sources in Africa are characterized rather differently from the other continents (Williams et al., 2009; Guenther et al., 2012; Giglio et al., 2013; Albrecht et al., 2016). Since Africa covers areas in both hemispheres with a large portion in the tropics, the atmospheric circulation over Africa experiences obvious seasonal changes induced by the seasonality of the ITCZ and the Hadley cell (Nicholson, 2008, 2009; Žagar et al., 2011; Suzuki, 2011). To cast some light on the seasonal variations of imported African ozone over Asia presented in this section, the ITCZ and ozone precursor emissions over Africa are discussed in section 3.2. Based on the discussion, the possible mechanisms that modulate the transport of African ozone to Asia are speculated in section 3.3.

带格式的: 字体颜色: 文字 1

~~4.1~~ 3.2 ITCZ and ozone precursor emissions over Africa

~~Referred to~~ Based on Nicholson (2009, 2013), Suzuki (2011), and Žagar et al. (2011), the mean positions of the ITCZ in Africa in the four seasons are approximately illustrated in Figs. ~~6a-6d~~ 8a-8d. The ~~seasonal~~ latitudinal migration of the ITCZ ~~between latitudes is a robust phenomenon and with season~~ varies with longitude (Nicholson, 2009; Suzuki, 2011). ~~The latitudinal shift and the migration is within a wider range of latitudes~~ in eastern Africa (10°E-40°E) than in western Africa (Figs. ~~6a-6d~~). ~~From boreal west of 10°E~~. In eastern Africa, ITCZ shifts between ~10°S in NH winter ~~to~~ and ~20°N in NH summer, while in western Africa, the center of the ITCZ swings from 40°N to 20°N in western Africa (Figs. ~~6a-6d~~), while in eastern Africa 5°N to 20°N between 40°E and 40°E, ITCZ shifts between ~~~10°S in boreal~~ 10°S in boreal NH winter and ~~~20°N in boreal~~ ~20°N in boreal summer (Figs. ~~6a-6d~~) within the NH.

带格式的: 字体颜色: 文字 1

带格式的: 字体颜色: 自动设置, 英语(加拿大)

带格式的: 左

带格式的: 字体颜色: 自动设置

带格式的: 字体颜色: 自动设置

带格式的: 字体颜色: 自动设置

带格式的: 字体颜色: 自动设置

Seasonal variations of African ozone and its seasonality largely depend heavily on biogenic ~~emissions, moderately on~~ biomass burning ~~and~~ lightning emissions, and ~~weakly on~~ anthropogenic emissions. The anthropogenic emissions are generally

~~considered to be~~ small and have weak seasonality (Aghedo et al., 2007; Williams et al., 2009). ~~The Based on the emission inventories in GEOS-Chem that are described in section 2.1, the~~ spatial distributions of ~~ozone precursor emissions are shown by season in Fig. 8, including~~ isoprene emissions from biogenic sources, CO emissions from biomass burning, and NO_x emissions from lightning ~~are shown by season in Fig. 6. The normalized seasonal at 700 and 300 hPa. Seasonal~~ variations of these emissions averaged over Africa, NHAF and SHAF are shown in Fig. 7. ~~The emission data are from the emission inventories in GEOS-Chem described in section 2.1. The normalized value equals to the original value minus the annual mean and then divided by the standard deviation.~~

~~As isoprene~~ Isoprene (C₅H₈) is the dominant non-methane volatile organic compound (NMVOC) emitted by vegetation (Marais et al., 2012) ~~and biogenic~~. Biogenic isoprene emissions in Africa ~~account~~ ~~are considered to be responsible~~ for about 65% of ~~ozone enhancement in~~ the African upper troposphere ~~ozone enhancement~~ (Aghedo et al., 2007), ~~isoprene~~. Isoprene emissions ~~are shown in Figs. 6a-6d as a8a-8d are~~ representative ~~of biogenic emissions of ozone precursor from biogenic sources-precursors. The magnitude and spatio-temporal pattern of the isoprene emissions in Africa in Fig 9 are comparable with Marais et al. (2014).~~ The maximum biogenic isoprene emissions are over central African rainforests throughout the year (Fig. 6a-6d Figs. 8a-8d). The seasonal cycle of biogenic isoprene over Africa peaks in ~~boreal~~ NH spring and ~~fall~~ autumn (Fig. 7a9a). Plenty of non-methane VOCs, ~~which may have relatively long lifetimes (such as methanol) or effective storage of NO_x (such as PAN), are~~ is emitted from biogenic sources that can be uplifted by strong convection (Tie et al., 2003). ~~Consequently, the contribution of, Aghedo et al. (2007) and Zare et al. (2014) suggested that~~ biogenic emissions ~~can lead to more~~ ozone ~~generation~~ in the African upper troposphere ~~is larger~~ than biomass burning and anthropogenic emissions (Aghedo et al., 2007; Zare et al., 2014).

In ~~boreal~~ NH winter, fires in Africa are active in the ~~Northern Hemisphere~~ NH between 0-10°N and 15°W to 40°E (Figs. 8e-8h, also see Sauvage et al., 2005). From ~~boreal~~ NH winter to ~~fall~~ autumn, regions with biomass burning ~~regions~~ shift southward

带格式的：英语(加拿大)

from central Africa to southern Africa (Figs. 8e-8h, Fig. 6, 2nd row, also see van der Werf et al., 2010; Giglio et al., 2013). In ~~the Southern Hemisphere~~ NH summer, fires are most active in ~~boreal summer~~ the SH from the equator to 20°S. Therefore, the regional CO emissions from biomass burning peak ~~in boreal~~ during NH winter in NHAF and ~~in boreal~~ during NH summer in SHAF (Fig. 7b9b). Aghedo et al. (2007) stated that biomass burning has the largest impact on surface ozone in the vicinity of the African burning regions during the burning seasons.

In Africa, lightning NO_x is produced mostly in the middle to upper troposphere (Figs. 6i-6p8i-8p, also see Pickering et al., 1998; ~~Ott et al., 2010~~; Miyazaki et al., ~~2014~~). Miyazaki et al. (2014) estimated that the ~~altitude~~ altitudes where the annual lightning NO_x ~~emission maximizes is~~ emissions maximize are around 11 km ~~for in~~ northern Africa and 9.36 km ~~for in~~ southern Africa. ~~Therefore,~~ Aghedo et al. (2007) suggested that lightning emissions mainly enhance ozone production in the African middle and upper troposphere (~~Aghedo et al., 2007~~). Ascribe to the high efficiency of deep moist convection, frequent lightning activities occur in the ITCZ (Christian et al., 2003; Avila et al., 2010). Collier and Hughes (2011) suggested that the peak lightning activities are generally located on the southern border of the ITCZ in Africa. The seasonality of the ~~locations for high geographic variation of~~ lightning NO_x ~~emission~~ emissions clearly shows the influence of ~~the solar declination and~~ the ITCZ over Africa (Collier and Hughes, 2011). When the ITCZ reaches to its northernmost position in ~~boreal~~ NH summer (Fig. 6e8c), lightning NO_x emission over ~~the~~ NHAF becomes the highest (Figs. 6, 7e9c and 7d9d). Similarly, the lightning NO_x emission over ~~the~~ SHAF peaks in ~~boreal~~ NH winter (Figs. 6, 7e9c and 7d9d).

4.23.3 Analysis of the mechanisms for the transport of African ozone to Asia

As African ozone mainly peaks in the Asian middle and upper troposphere, the horizontal distributions of African ozone at 400 hPa in January, April, July, and October overlaid with winds are shown in Fig. 10 to illustrate the seasonality and the transport pathways based on GEOS-Chem simulations of African ozone to Asia at this level. In NH winter, African ozone can be transported for a long distance along the subtropical

带格式的：正文

westerlies in the two hemispheres, reaching the western Pacific in the NH and across Australia in the SH, respectively. In NH summer, the NH subtropical westerlies and tropical easterlies shift to their northernmost positions; less African ozone can be transported to Asia than in the other seasons. Furthermore, Fig. 11 shows the latitude-altitude cross sections of African ozone and winds averaged from 0 to 40°E. This is to show how African ozone in the source region varies vertically along different latitudes. Fig. 12 is the same as Fig. 11 but for the longitude-altitude cross sections averaged from 20°N to 35°N so to show the transport pathway along longitude from Africa to Asia. Fig. 13 shows the 20-year mean paths for the trajectories that run from seven representative sites (Cairo, Ghat, Abuja, Khartoum, Juba, Dar es Salaam, and Luanda) to Asia. The mean paths are shown by season and by the original tropospheric layer, including the lapse day from the beginning of the trajectories. Additionally, we conduct three sensitivity experiments by switching off the biogenic, lightning, and biomass burning emissions, respectively, to assist our analysis. The separate contributions of the three sources to tropospheric ozone over Africa are shown in Fig. S7. In the following, we analyze the information from these figures, in combination with literature, to explore possible mechanisms responsible for the transport of African ozone to Asia in the four seasons.

带格式的: 字体颜色: 自动设置

3.3.1 In NH winter

In NH winter, the eastern part of ITCZ shifts to its southernmost. Fig. 8 shows the latitude-altitude cross sections of African ozone and wind fields averaged from 0 to 40°E. Fig. 9 is the same as Fig. 8 but for the longitude-altitude cross sections averaged from 25°N to 35°N. In Fig. 10, vertical distributions of African ozone fluxes along the western border and eastern border of Asia are shown by season. Apparently, the inflow fluxes are larger than the outflow fluxes throughout the year. Controlled by the northern subtropical westerly jet, imported African ozone fluxes peak in the upper troposphere. The latitudes where African ozone flux peak vary with the seasonal

~~swing of the northern subtropical westerlies.~~

~~In boreal winter, deep convection, strong convergence in the lower troposphere can be seen from 10°S to 20°S (Fig. 8a), indicating the position of the ITCZ in the Southern Hemisphere. Thein eastern Africa around 15°S (Figs. 8a and 11a), while the western part of the ITCZ remains in NHAF around 5°N (Figs. 8a and 11a). In Fig 11a, the ITCZ around the two latitudes and the two cells of the Hadley circulation are clearly shown as well. Due to . Biomass burning is active in NHAF (Figs. 8e and 9b). Biogenic emissions (Fig. 9a) and NO_x emissions from lightning (Fig. 9c) are the highest in SHAF. All these conditions are well reflected in Fig. 11a. The elevated African ozone in the NHAF lower troposphere from the equator to 10°N is resulted from high biomass burning and biogenic emissions (Figs. 8a and 8e, also see Figs. S7a and S7c, Aghedo et al., 2007), only this ozone is mostly confined under 700 hPa. In contrast, the high ozone concentrations over the SHAF middle and upper troposphere are due to deep convection and strong convergence of the ITCZ in SHAF that brings biogenic precursors to the upper troposphere and enhance ozone production there (Fig. 8a, also see S7a). In addition, ozone can be also generated in the middle and upper troposphere due to frequent lightning activities, the region with high ozone appears over the ITCZ in the African middle and upper troposphere in the Southern Hemisphere. In the lower troposphere, ozone concentrations are high from the equator to 10°N, resulting from high biomass burning emissions as discussed in section 4.1 (Aghedo et al., 2007). This ozone is uplifted (Fig. 8a, 0–10°N) by the ITCZ in the Northern Hemisphere (Figs. 6a and 6e). (Fig. 8i, also see Fig. S7b, Aghedo et al., 2007).~~

Driven by the Hadley cell, African ozone in NHAF is transported upward over the ITCZ, northward in the middle and upper troposphere, and equatorward in the lower troposphere, upward over the ITCZ, poleward in the middle and upper troposphere. The northward outflowflow in the middle and upper troposphere gradually becomes weaker and weakerweakens between 15–30°N (Fig. 8a). Eventually, carried by the 11a) where air parcels merge into the NH westerlies. This is also seen in the HYSPLIT trajectories in Figs. 13a and 13b. The trajectories originated from the two sites in the SH stop moving northward and turn toward the east around 20°N (Figs. 13a and 13b).

From the source region to the receptor region, the NH subtropical westerlies, African ozone is transported eastward to Asia (Fig. 9a, also see Fig. build the pathways (Fig. 12a in section 4.4), also see trajectories in Figs. 13a and 13b). In Fig. 12a, along the latitudinal pathways, downdrafts behind the European trough around 40°E divert part of African ozone to the surface. However, the updrafts ahead of the European trough favor the uplift of African ozone so it can be transported for long distance in the upper troposphere.

Finally, over the receptor region Asia, the downdrafts behind the Asian trough situated at around 140°E bring African ozone from the upper layers to the lower layers,

带格式的: 字体颜色: 自动设置

Consequently, the contribution of African ozone to Asia becomes the highest in the middle and upper troposphere (see Figs. 2b5 and 3a for 6). In NH winter, the transport of African ozone to Asia generally takes 4-6 days varying with altitude and latitude (Figs. 13a and 13b).

3.3.2 In NH spring

In NH spring, a region with high ozone concentrations, and above 40 ppbv appears in higher altitudes and extends to a larger area in the middle and upper troposphere than in NH winter (Figs. 11b and 12b). This region is further north than the elevated ozone region in NH winter. This is because the ITCZ in eastern Africa shifts northward to near the equator (Fig. 40a for inflow ozone flux). During 8b). Biomass burning is least active in both NHAf and SHAF (Figs. 8f and 9b) while the biogenic emissions in the season are the largest in NHAf and the second largest in SHAF (Fig. 9a). As the ITCZ is over the region where biogenic emissions are also high near the equator (Fig. 8b), The ITCZ effectively uplifts the biogenic precursors and also leads to production of NO_x from lightning in the upper layers (Fig. 8j). The ozone precursors from both sources can enhance the generation of ozone in the middle and upper troposphere (Figs. S7d and S7e, also see Aghedo et al., 2007) where elevated ozone concentrations are apparent (Fig. 11b). Therefore, more African ozone can be exported out of Africa in the upper troposphere

带格式的: 字体颜色: 黑色

in NH spring than in NH winter (Fig.10a vs.10b, Fig.12a vs.12b). It takes more time for trajectories to arrive Asia in NH spring than in NH winter (Fig. 13a-13c vs. 13d-13f).

3.3.3 In NH summer

In NH summer, the ITCZ in Africa swings to its northernmost position around 15°N (Figs.8c and 11c).The region with active biomass burning shifts to SHAF (Figs. 8g and 9b). A large amount of ozone, generated from the biomass burning in SHAF, is shown in Fig. 11c over the SHAF lower troposphere from ~15°S to the equator. However, this ozone is mostly confined in the lower troposphere (Figs. 11c and S7i). Note that ozone in the middle and upper troposphere north of 15°N is higher than in the other seasons, which is likely resulted from lightning activities and biogenic emissions (Figs. 8k, S2 and S7g). This ozone can be readily transported to Asia.

Along the transport pathway from Africa to Asia (Fig. 12c), Africa ozone concentrations at the source region are the highest among the four seasons (Figs. 10c and 12c). However, meteorological conditions along the pathway are most unfavorable for the transport of African ozone to Asia because of multiple reasons. First, the NH subtropical westerly jet in NH summer moves the northernmost position to around 40°N (Huang et al., 2012). The tropical easterlies also shift northward along (Fig. 8c) so to prevent African ozone from reaching Asia between 10°N and 30°N in the middle and upper troposphere (see Figs. 5 and 6 for imported African ozone concentrations, Figs. 10c and 12c for African ozone and wind fields). Second, on the transport pathway, the heavy downdrafts from the Saharan High, a midtropospheric high-pressure system that is an eastward extension of the Azores High (Nicholson, 2017) and the Arabian High in the middle troposphere over Middle East (Liu et al., 2011) hamper African ozone from reaching Asia. Note in Fig. 12c, there is a region with lower African ozone than its surrounding in the lower troposphere between 10°E and 40°E. The downwards of African ozone near 30°E is likely due to a summertime trough at 40°E (Zhu et al., 2017b). Consequently, the amount of African ozone is

带格式的：左，首行缩进：0 字符

reduced during the transport. Thirdly, in the source region, strong updrafts occur over the Tibetan Plateau (Fig. 12c) and further block the transport of African ozone toward the east. Finally, the strong divergence outflow in the Southern Hemispheric upper troposphere carries African ozone (Fig. 8a, 500–200 hPa, 10–20°S) to the Asian upper troposphere, contributing to 2–3 ppbv ozone, which is 30% of the total from the South Asia High obstructs the eastward transport of African ozone in the upper troposphere. For these reasons, imported African ozone over Asia (Figs. 4e and 4d) is lowest in NH summer among the four seasons (Figs. 5 and 6). There are scarcely any trajectories from the African sites that can cross Asia, unlike in the other seasons (Figs. 13g, 13h, and 13i).

3.3.4 In NH autumn

In NH autumn, the ITCZ shifts southward to a location similar to in NH spring (Fig. 8b vs. 8d). Biogenic emissions are slightly lower than in NH spring (Fig. 8b vs. 8d, Fig. 9a), whereas lightning NO_x emissions are higher than in NH spring (Fig. 8j vs. 8l, Fig. 9c). In boreal spring, a region with high ozone concentrations (>40 ppbv) appears in higher altitudes and extends to a larger area in the middle and upper troposphere than in boreal winter (Figs. 8b and 9b) mainly due to the highest biogenic emissions in the NHAf (section 4.1, Figs. 6b and 7a). The region is also further north than in boreal winter under the influence of seasonal migration in the locations of the ITCZ and consequently the lightning. Ozone in the African lower troposphere becomes lower than in boreal winter, likely due to weaker biomass burning activities in the central Africa (Duncan et al., 2003). In general, the pathways for African ozone to be transported to Asia in boreal spring are similar to those in winter (Figs. 5a vs 5b, 8a vs 8b, 9a vs 9b, 10a vs 10b). In the upper troposphere, however, more ozone is transported to Asia in boreal spring than in boreal winter (Fig. 3a), mainly due to the seasonal increase of biogenic emissions (Fig. 7a).

In boreal summer, African ozone in the lower troposphere peaks from $\sim 15^\circ\text{S}$ to the

带格式的: 字体颜色: 黑色

带格式的: 字体颜色: 黑色

equator (Fig. 8c), corresponding to the biomass burning emissions (Figs. 6g and 7b). However, because the center of the ITCZ shifts to $\sim 20^{\circ}\text{N}$ over the Sahara (Fig. 6c), ozone generated from biogenic emissions is uplifted less effectively than in the other seasons (Fig. 8c vs 8a, 8b, and 8d). Consequently, ozone in the African middle and upper troposphere south of 15°N is lower than in the other seasons (Fig. 8c). However, resulting from the northward migration of lightning activities, ozone in the middle and upper troposphere north of 15°N is higher than in the other seasons (Fig. 8c). The transport of African ozone to Asia in boreal summer differs from that in boreal winter. In boreal summer, the updrafts over the Tibetan Plateau are strong (Fig. 9e), which serves as a heat source for the Asian summer monsoon (Wu et al., 2012, 2015) and blocks the transport of African ozone to Asia (Fig. 9e). Furthermore, the northern westerly jet moves northward to around 40°N (Huang et al., 2012). Biomass burning is strong but occurs mostly in SHAF (Fig. 9b) so that it imposes small influence on the Asian troposphere (Fig. 7). In NHAF, the strong biogenic emissions are uplifted effectively by the ITCZ, similar to NH spring. The uplifted biogenic precursors and NO_x from lightning in the middle and upper troposphere lead to elevated ozone there (Fig. 11d, see also Figs. S7j and S7k). African ozone concentrations in the NHAF middle and upper troposphere look higher than in NH spring (Fig. 10b vs. 10d, Fig. 11b vs. 11d, Fig. 12b vs. 12d). However, there is less African ozone arriving Asia in NH autumn than in NH spring (Figs. 5 and 6). This may be due to two reasons. In NH spring, the elevated African ozone in NHAF is located in higher altitudes than in NH autumn (Fig. 11b vs. 11d, Fig. 12b vs. 12d). This ozone can be more effectively transported to Asia by more speedy winds in the upper layers. The second reason is because of the weaker subtropical westerlies in NH autumn than in NH spring (Fig. 10b vs. 10d, Fig. 12b vs. 12d, also see Huang et al., 2012). The transport pathways and the time for the transport of African ozone to Asia in NH autumn are similar to in NH spring, as shown in the trajectories (Fig. 13).

4 Meteorological influences ~~The tropical easterlies also shift northward along (Fig. 5e) and further prevent African ozone from reaching Asia between 10°N and 30°N~~

带格式的: 字体颜色: 黑色

带格式的: 字体颜色: 黑色

above the lower troposphere (see Figs. 2a-2d, and 3a-3b for imported ozone concentrations, Fig. 10c for inflow ozone flux).

In boreal autumn, the locations of the ITCZ and the Hadley cell are similar to these in boreal spring (Figs. 8b vs 8d). Ozone in the African middle troposphere is higher in boreal autumn than in boreal spring, attributed to stronger lightning NO_x emission (Figs. 7c and 7d). However, because of the weaker zonal winds (Figs. 9b vs 9d), the ozone inflow to Asia is smaller than in spring (Figs. 10b vs 10d).

Overall, the influence of African ozone on the Asian middle and upper troposphere is mainly attributed to ozone transport driven by the Hadley circulation and subtropical westerlies. The seasonality of the ITCZ, the Hadley cell, and the westerlies can greatly influence the seasonality of the pathways of ozone transport from Africa to Asia.

4.3 Interhemispheric transport of ozone from the SHAF to Asia

In the upper troposphere, the horizontal distribution of SHAF ozone at 200 hPa in January is shown in Fig. 11a. SHAF ozone in Asia is 2–3 ppbv along 60°N–150°E between 0–30°N (Fig. 11a). Because of the ITCZ and the Hadley circulation, a part of SHAF ozone is inter-hemispherically transported to the Northern Hemisphere (Fig. 8a). Then, driven by northern subtropical westerly jet, this ozone can finally reach Asia (Fig. 11a). Over Asia, ozone from SHAF is the largest in boreal winter than in the other seasons in the upper troposphere, while in the lower troposphere, it is the largest in summer than in the other seasons (Figs. 4c and 4d). Fig. 11b shows SHAF ozone in July at 925 hPa, with concentrations of 2–6 ppbv over the Arabian Sea and the west coast of the Indian subcontinent. This ozone is transported to India in boreal summer by the Somalia cross-equatorial flow (Fig. 11b), which is the strongest seasonal cross-equatorial flow in the lower troposphere (Halpern and Woiceshyn, 1999, 2001). This is the reason for the summer maximum of African ozone (~4 ppbv) over the Asian lower troposphere south of 15°N (Fig. 2c). This transport is also captured in Fig. 10e as the influx of Africa ozone in the Asian lower troposphere south of 15°N.

4.4 Analysis of the transport pathways based on trajectory statistics

In this section, we use six-day forward trajectories to further analyze the pathways for ozone transport from Africa to Asia. Fig. 12 shows the clustered six-day forward trajectories during 1987–2006 starting from Cairo (31°E , 30°N), Abuja (7.4°E , 9°N), Dar-es-Salaam (39°E , 6.8°S), and Johannesburg (28°E , 26.2°S) in the lower, middle and upper troposphere, respectively. The four sites are chosen for different latitudes in Africa.

In boreal winter, in NHAF, 40% of the 6-days trajectories in the lower troposphere from Cairo flow to higher latitudes in Asia (Fig. 12c). In the middle troposphere, 74% trajectories from Cairo reach Asia along the northern subtropical westerlies (Fig. 12b). Approximately, 10% trajectories from Abuja reach Asia following a pathway of upward along the northern Hadley cell and then eastward along the northern subtropical westerlies (Fig. 12b). In the upper troposphere, African ozone can be transported to Asia fast and with longer distances within 6 days (Fig. 12a). After reaching Asia (across 60°E), most of the trajectories in the middle and upper troposphere move downwards along the westerlies (Figs. 12a and 12b). Driven by the northern subtropical westerly jet, 98% trajectories from Cairo and about 41% trajectories from Abuja can reach Asia (Fig. 12a). Toward to further south, Dar-es-Salaam is mainly under the influence of the tropical easterlies and the south subtropical westerlies in the lower and middle troposphere so that the trajectories from this site are either westwards or eastwards along the westerlies in the Southern Hemisphere (Figs. 12b and 12c). However, in the upper troposphere, about 25% trajectories at the site flow to Asia (Fig. 12a) due to the convective divergence over the ITCZ. At Johannesburg in the southern Africa, nearly no trajectories can reach Asia (Figs. 12a–12c).

In boreal summer, induced by the northward shift of the northern subtropical westerlies ($\sim 40^{\circ}\text{N}$), fewer trajectories reach Asia than in winter (Figs. 12d–12f). Because of the northward shift of the Hadley cell and the tropical easterlies, trajectories from Abuja travel westward in the middle and upper troposphere, while in the lower troposphere, the trajectories run around locally (Figs. 12d, 12e, and 12f).

Similar to winter, no trajectories from Johannesburg reach Asia because of the southern location of the site (Figs. 12d, 12e, and 12f). However, at Dar es Salaam in east Africa, there are ~14% trajectories in the lower troposphere that travel toward India (Figs. 12e and 12f) under the influence of Somali jet (Halpern and Woiceshyn, 1999, 2001; Lal et al., 2014). The Somali jet can transport ozone from the east coast of Africa to Asia, resulting in a summer maximum of African ozone over the Asian lower troposphere south of 15°N (Fig. 2e for ozone concentration, and Fig 10e for the ozone inflow flux). Overall, the analysis of the trajectory statistic agrees well with the GEOS-Chem simulations discussed in section 4.2.

4.5 Influences of the ITCZ on the interannual variation of the transport of African ozone transport to Asia in boreal winter

~~As known, the deep convection along the ITCZ can carry ozone precursors from biogenic, biomass burning, and anthropogenic emissions to upper levels. The ITCZ is also a zone with large lightning activities. The convective divergence in the upper troposphere over the ITCZ plays a significant role in ozone outflow and the interhemispheric transport between SHAF and NHAF. Therefore~~**4.1 The influence of the ITCZ on African ozone transport to Asia in NH winter**

As discussed, the ITCZ can impact meteorology in Africa (Sultan and Janicot, 2000; Xie, 2004; Hu et al., 2007; Collier and Hughes, 2011; Suzuki, 2011). The deep convection along the ITCZ can carry ozone precursors from biogenic, biomass burning, and anthropogenic emissions to the upper layers from the surface. The ITCZ is also a zone with large lightning activities and thus can impact the seasonality of ozone precursor emissions (for example, NO_x emission from lightning). To explore, The convective divergence in the ~~role that~~ upper troposphere over the ITCZ in Africa plays ~~in~~ a significant role in output of African ozone and in the interhemispheric transport from Africa between SHAF and NHAF (Fig. 11 and see trajectories in Fig. 13).

To investigate the impact of ITCZ on the interannual variation of the transport of African ozone to Asia, we use the monthly Outgoing Longwave Radiation (OLR) data

带格式的: Sub1 Char, 字体: 加粗, 字体颜色: 文字 1

带格式的: Sub1

带格式的: Sub1 Char, 字体颜色: 文字 1

带格式的: 字体颜色: 自动设置

带格式的: 左, 缩进: 首行缩进: 1 字符

from NCAR at $2.5^\circ \times 2.5^\circ$ with temporal interpolation (Liebmann and Smith, 1996) as a proxy for convective activity in the tropics to describe the intensity of ITCZ, similar to previous studies (Waliser et al., 1993; Mounier and Janicot, 2004; Fukutomi and Yasunari, 2013, 2014). According to Waliser et al. (1993) and Fukutomi and Yasunari (2013), the number of the grid points with OLR ≤ 260 W/m² in the region of 15°W-45°E, 20°S-20°N can indicate the intensity of the convection over the ITCZ in Africa.

We find that intensity of ITCZ in Africa is mostly related to imported African ozone over Asia in NH winter. Fig. 1314 shows the time series of anomalies of imported African ozone from Africa, NHAF and SHAF, averaged over Asia, against the intensity of the ITCZ over Africa (after normalization. The intensity of the ITCZ is normalized, i.e., the normalized value is equal to the original value minus the mean that is and then divided by the standard deviation) in January from 1987 to 2006. The anomalies of imported ozone from SHAF are quite small in the lower and middle troposphere (Fig. 4), so the time series is not shown. Positive correlations are found between the intensity of the ITCZ and anomalies of imported African ozone over Asia, are correlated with the correlation coefficient (r) being of 0.61, 0.46, and 0.64 for the Asian lower (975 hPa), middle (600 hPa), and upper (200 hPa) troposphere, respectively, all statistically significant at the 95% level ($p < 0.05$). Significant

带格式的: 字体: 倾斜

Separating by the hemisphere, significant correlations are also found between the ITCZ and imported NHAF and SHAF ozone in the entire troposphere in Asia (Fig. 14). The interhemispheric transport of ozone from SHAF to Asia also correlates with the intensity of ITCZ in Africa well, with r being 0.56 in the Asian upper troposphere (Fig. 13a). In boreal winter, the center of the ITCZ is located in the upper region of biogenic (14a). The interhemispheric transport to Asian middle and biomass burning emissions (Figs. 6a and 6e). When lower troposphere is little so their time series are not shown.

Overall, when the intensity of the African ITCZ is stronger, more ozone and ozone precursors are uplifted to the middle and upper troposphere and transported poleward/northward and then eastward to Asia by the northern NH subtropical

带格式的: 左

westerlies (Figs. 12a-12e). Additionally, driven by the enhanced convective divergence over the ITCZ, the interhemispheric transport more ozone from SHAF increases in is transported across the equator and to the NHAF upper troposphere (Figs. 8a and 13a). Consequently, transport of African ozone from Africa to Asia increases in the Asian middle and upper troposphere. At the same time Meanwhile, carried by the downdrafts from the Asian winter monsoon (Figs. 9a, 12a-12e Zhu et al., 2017b), more ozone is transported to the surface in Asia (Zhu et al., 2017b).

5 An overview 4.2 The influence of meteorology on the interhemispheric transport of African ozone from SHAF to Asia

The processes discussed in section 4 on the transport of African ozone to Asia can be briefly summarized for boreal winter (Fig. 14a) and boreal summer (Fig. 14b), respectively, from perspectives of both the atmospheric circulations (Xie, 2004; Mari et al., 2008; Nicholson, 2009; An et al., 2015; Ding et al., 2015; Li et al., 2016; Nützel et al., 2016) and emissions of ozone precursors (Aghedo et al., 2007; Marais et al., 2012; Giglio et al., 2013; Miyazaki et al., 2014; Zare et al., 2014; Albrecht et al., 2016).

During boreal winter, the Hadley cell and the northern subtropical westerlies build the transport pathways from Africa to Asia. Formed at the ascending branch of the Hadley circulation, the location of the ITCZ over Africa shows different characteristics in Africa west of 10°E and Africa east of 10°E (Nicholson, 2009). Over the ITCZ, a great amount of latent heat is released by deep convection, which drives the ascending branch of the Hadley circulation (Xie, 2004). The biomass burning emissions are mainly in the Northern Hemisphere (Fig. 6e), which contributes to the production of a significant amount of African ozone in the lower troposphere (Fig. 8a, also see Mari et al., 2008). The ozone precursors can be carried upward from the surface to the upper layers by the rising branch of the Hadley circulation.

In the African middle and upper troposphere, vigorous convection within ITCZ clouds results in strong thunderstorms, accompanied with much lightning (Avila et al., 2010). Based on the C-shaped vertical profile of the lightning-generated NO_x,

带格式的: 字体颜色: 自动设置

带格式的: Sub2

带格式的: 字体颜色: 自动设置

带格式的: 字体颜色: 自动设置

带格式的: 字体颜色: 自动设置

lightning activities contribute to the generation of a large proportion of ozone in the African middle and upper troposphere (Fig. 8a, also see Pickering et al., 1998; Miyazaki et al., 2014). Then ozone generated from chemical reactions and convection uplifting is transported poleward by the convective divergence over the ITCZ and downward by the descending branch of the Hadley cell. The northern subtropical westerlies carry African ozone to Asia in the middle and upper troposphere. Overall, in boreal winter, African ozone is mainly produced from biogenic and lightning sources (Aghedo et al., 2007; Zare et al., 2014) and is transported to Asia mostly in the middle and upper troposphere, governed by the northern Hadley cell and subtropical westerlies.

In boreal summer, the ITCZ and the Hadley circulation move northward in response to the solar heating to the Northern Hemisphere. The African easterly jet, tropical easterly jet and northern subtropical westerly jet all shift northward as well. However, the fire areas shift southward to the Southern Hemisphere (Clain et al., 2009; Giglio et al., 2013). Therefore, the ITCZ can facilitate lightning NO_x production in NHAF but uplifts little ozone generated from biomass burning. In the upper troposphere, transport of African ozone to Asia is hampered by the SAH, a prevailing weather system over Eurasia in boreal summer (Nützel et al., 2016). The updrafts associated with SAH prevent African ozone from reaching Asia at low latitudes ($<30^\circ\text{N}$) (Fig. 9c). In the meantime, the easterlies prevail south of 30°N so to block African ozone from reaching Asia. Overall, both the meteorology and emissions in boreal summer weaken the transport of African ozone to Asia in the middle and upper troposphere. Noticeably, the Asian summer monsoon (Zhang et al., 2002; Ding et al., 2005) is in favor of transport of African ozone to Asia in the lower troposphere. Located north to the enhanced Mascarene Anticyclone, on the east coast of Somali, Somali cross-equatorial flow served as an essential component of the Asian monsoon system (Joseph and Sijikumar, 2004). Peaked at 925 hPa (Zhu, 2012), the Somali jet carries ozone in eastern Africa to India in the lower troposphere (Figs. 10e and 11b).

6 Conclusions

The transport of ozone originated in the African troposphere to Asia is investigated through the analysis of the simulations using a global chemical transport model, GEOS-Chem, and a trajectory model, HYSPLIT. This study shows that imported African ozone varies greatly with latitude, longitude, and altitude in the Asian troposphere, also with strong seasonality. In the Asian upper troposphere, imported African ozone is the largest during February–May (>10 ppbv) and the lowest during July–September (<6 ppbv). In the middle troposphere, imported African ozone is at a maximum from December to April (>10 ppbv) and at a minimum from June to September (~ 4 ppbv), slightly different from the seasonality in the upper troposphere. In the lower troposphere, the African influence is small (<6 ppbv), with a maximum from December to February ($>6\%$) and a minimum from September to November ($<5\%$). Overall, the maximum influence of African ozone is in boreal winter and early spring in the middle and upper troposphere of southern Asia (5°N – 40°N). Ozone from NHAf makes up over 80% of the total imported African ozone in most seasons and layers in Asia, except over the upper troposphere in boreal winter and over the lower troposphere in summer, when the interhemispheric transport of ozone from SHAF becomes stronger than in the other seasons at the same layers.

The underlying mechanisms for these seasonal variations in the transport of African ozone to Asia are explored. In boreal winter, facilitated by ITCZ, ozone produced from its precursors from biogenic and biomass burning sources can be efficiently lifted up to high layers. The uplifted African ozone is transported poleward by the Hadley circulation in the upper troposphere and then eastward by the subtropical westerlies in the middle and upper troposphere. The convective divergence over the ITCZ (the poleward branch of the Hadley circulation) in the Southern Hemisphere promotes the interhemispheric transport of SHAF ozone, resulting in a contribution of SHAF ozone of 2–3 ppbv in the upper troposphere, larger than in the other seasons. Under the influence of both the Hadley circulation and subtropical westerlies, African ozone peaks mainly in the Asian middle and upper troposphere. In boreal summer, as the northern westerlies shift northward, African ozone is mostly transported to the Asian

~~upper troposphere around 40°N. In the lower troposphere, the Somali jet serves as another important pathway for the interhemispheric transport of SHAF ozone, carrying ozone from eastern Africa to India and thus forming a summer African ozone maximum in the lower troposphere over latitudes south of 15°N.~~

~~The interannual variation in African ozone transport to Asia is greatly influenced by the intensity of the ITCZ in boreal winter. As shown in Fig. 7 and discussed in earlier sections, ozone generated in SHAF can be transported across the equator and eventually to Asia. This is illustrated in more detail in Fig. 15, showing seasonal-altitude variations of imported ozone from NHAF and SHAF over Asia and the fractional contributions of NHAF and SHAF ozone to the total imported African ozone. Ozone from NHAF accounts for over 80% of the total imported African ozone in the Asian tropospheric column throughout the year, except for in the upper troposphere during NH winter and in the lower troposphere during NH summer (Figs. 15b and 15d). This represents two important interhemispheric transport pathways.~~

~~For the first transport pathway, Fig. 7 suggests that the SHAF ozone originates mainly from the SHAF UT. This ozone can be transported northward across the equator along the Hadley circulation and then eastward to Asia by the NH subtropical westerlies (Fig. 13a). The amount of ozone being transported is at the maximum in NH winter and at the minimum in NH summer (Figs. 7 and 15c) when the ITCZ is at its southernmost and northernmost position, respectively (Figs. 8a-8d). This can be further illustrated in the horizontal distribution of SHAF ozone at 200 hPa (Fig. 16a). SHAF ozone is 2-4 ppbv over China south of 30°N and 4-6 ppbv over western India. As shown in section 4.1 (Fig. 14a), the variation of the ITCZ intensity in Africa can explain 31% the interannual variation of the transport of SHAF ozone to the Asian in NH winter along this pathway.~~

~~The second transport pathway is shown in Fig. 16b for SHAF ozone distribution at 850 hPa in July, as Fig. 7c also suggests that the interhemispheric transport mainly occurs from the SHAF lower and middle troposphere. SHAF ozone concentrations are 2-4 ppbv over the Arabian Sea and the west coast of the Indian subcontinent. This ozone is transported to India in NH summer by the Somali cross-equatorial flow (Fig.~~

16b), which is the strongest seasonal cross-equatorial flow in the lower troposphere, serving as an essential component of the Asian monsoon system (Zhu, 2012). This is the reason for the maximum SHAF ozone (~4 ppbv) over the Asian lower troposphere south of 10°N in NH summer (Fig. 5c). One more evidence for this transport is shown in the trajectories from Dar es Salaam, eastern coast of Africa (Figs. 13h and 13i). The interhemispheric ozone transport to western India takes more than 6 days. Furthermore, the signal of the transport is captured in the ozonesonde data in western India. The vertical distributions of the seasonal ozone variations at Poona and Thiruvananthapuram are shown for the ozonesonde and GEOS-Chem data (Fig. 4). A dip of lower tropospheric ozone concentrations in both data is apparent in NH summer, when the Somali jet carries clear air masses from sea which can be traced back to SHAF (Figs. 13h, 13i and 16b).

To search for a connection between the Somali jet and the imported SHAF ozone over western India, we use an index, proposed by Li et al. (2014a), to indicate the intensity of the Somali jet. The index is calculated as the mean meridional wind at 850 hPa in the domain shown in Fig. 16b. Li et al. (2014a) correlated the Somali jet and other cross-equatorial flows with the index. Fig. 17 shows the anomaly of SHAF ozone averaged in the lower troposphere at Poona and Thiruvananthapuram during NH summer from 1987 to 2006. Positive correlations are found between the anomaly and the intensity of the ITCZ in Africa Somali jet at both sites with the correlation coefficients over 0.56, significantly at the 95% level.

5 Discussion and the interannual variations conclusions

We have characterized the transport of African ozone to Asia according to the simulations of a global chemical transport model, GEOS-Chem, for 20 years from 1987 to 2006. The ozone generated in the African troposphere is tracked using the tagged tracer simulation with GEOS-Chem. Combining with analysis of trajectory simulations using HYSPLIT and meteorological data of winds and OLR, we draw conclusions with discussion as follows.

1. In Asia, imported African ozone over Asia shows strong seasonality that varies

带格式的: 字体颜色: 文字 1

带格式的: 字体颜色: 文字 1

带格式的: 字体颜色: 文字 1

带格式的: 字体颜色: 文字 1

带格式的: 字体颜色: 文字 1

greatly with latitude, longitude, and altitude in the troposphere (Figs. 5- 6). The influence of African ozone mainly prevails in Asia south of 40°N. From 5-40°N, imported African ozone is largest from March to May (10-16 ppbv) and lowest during July-October (2-6 ppbv) in the Asian upper troposphere (Fig. 5a). In the middle troposphere, imported African ozone is at a maximum from January to March (10-16 ppbv) and at a minimum from July to September (2-4 ppbv). Near the surface, the African influence is small (below 6 ppbv). Overall, the influence of African ozone peaks in the Asian middle and upper troposphere between 20°N and 30°N in NH winter and spring. Over 5-40°N, the mean fractional contribution of imported African ozone to the overall ozone concentrations in Asia is largest during NH winter in the middle troposphere (~18%) and lowest in NH summer throughout the tropospheric column (~6%).

2. Both the tagged ozone and the trajectory simulations show that the Hadley cell connects the subtropical westerlies to form a transport route from Africa to Asia (Figs. 10-13). This is a primary pathway that occurs throughout the year. It takes 4-6 days for African ozone to reach Asia depending on the season and the initial altitude and latitude of the airmass, i.e., faster in NH winter than in NH summer, faster in higher altitudes than in lower altitudes, and faster in higher latitudes than in lower latitudes (Fig. 13). The second transport pathway only appears in NH summer that runs from eastern Africa near the equator to the Indian low troposphere (Figs. 13h and 13i). It takes 6 or more days for African ozone to reach Asia along this pathway.

3. The seasonality of African ozone influence on Asia results from the collective effects of meteorology, chemistry, and ozone precursor emissions in the source and receptor regions and between them. For the primary transport pathway, ozone and ozone precursors from various sources in Africa can be efficiently lifted up to high altitudes by the ITCZ. The African ozone in the middle and upper troposphere can be transported northward along the upper branch of the Hadley circulation and then eastward to Asia along the NH subtropical westerlies in the middle and upper troposphere. Therefore, the seasonal swings

带格式的

of the Hadley cell and NH subtropical westerlies play a dominant role in determining the seasonality of this transport pathway. Consequently, imported African ozone in Asia is least in NH summer, increasing toward both NH spring and NH autumn. In NH spring, there are more biogenic and lightning NO_x emissions than in NH winter. These precursors are uplifted by the ITCZ, making more ozone in the upper layers than in NH winter. Consequently, there is more African ozone to be transported to the Asian upper troposphere in NH spring than in winter (Figs. 5a and 6a). Although more ozone appears in Africa in NH autumn than in spring, there is less imported African ozone over Asia in NH autumn than in spring (Figs. 5 and 6a), likely due to the facts that the elevated ozone in NHAf is located in higher altitudes in NH spring and the NH subtropical westerlies are stronger in NH spring. In NH summer, although the ozone outflow from Africa is high, the ozone hardly reaches Asia because of the blockings of Saharan High, Arabian High, and Tibetan High along the transport pathway in the middle and upper troposphere, in addition to the northward swing of the westerlies. Finally, the ITCZ in Africa, combining with the geographic variations in ozone precursor emissions with season, can modulate the seasonality of transport of African ozone to Asia. When the ITCZ coincides with the ozone precursor emissions from biogenic and biomass burning emissions, in addition to enhanced NO_x emissions from lightning, strong ozone export out of Africa can be resulted, such as in NH spring.

带格式的: 英语(加拿大)

4. The interannual variation of the transport of African ozone to Asia is closely related to the intensity of the ITCZ in Africa in NH winter. Positive correlations are found between the intensity of the ITCZ in Africa and imported African ozone over Asia ($r = 0.64$ at 200 hPa, $r = 0.46$ at 600 hPa, and $r = 0.61$ at 975 hPa). Greatly influenced by the proximity of the ITCZ to the biogenic, biomass-burning and anthropogenic emissions, the uplifting of ozone and its precursors from the surface to higher altitudes is much more effective in boreal winter than in boreal summer., and $p < 0.05$ for the three layers) (Fig. 14). The stronger the ITCZ in Africaa NH winter is, the more ozone and its precursors from the surface

带格式的: 字体: 倾斜

带格式的: 字体: 倾斜

带格式的: 字体: 倾斜

emissions can be uplifted. In the ~~meanwhile, meantime, more~~ lightning NO_x is produced ~~in the middle and upper troposphere. Additionally, the convective divergence over the ITCZ in the upper troposphere is enhanced, resulting in increased.~~ Furthermore, the interhemispheric transport of ozone from SHAF is enhanced. Consequently, more African ozone can be transported to Asia ~~by~~.

5. Ozone from NHAF makes up over 80% of the subtropical westerlies total imported African ozone in the middle Asian troposphere in all layers and seasons, but with two exceptions in which ozone from SHAF becomes larger than 20% of the total imported African ozone (Figs. 7 and 15). The first exception occurs in the Asian upper troposphere.

带格式的: 字体颜色: 文字 1

带格式的: 字体颜色: 文字 1

带格式的: 字体颜色: 文字 1

带格式的: 字体颜色: 文字 1

during NH winter, corresponding to the primary transport pathway in NH winter (Fig. 7). In the season, the ITCZ swings to its southernmost position in Africa and the convective divergence over the ITCZ in the upper troposphere is enhanced, resulting in more interhemispheric transport of ozone from SHAF. The interhemispheric transport along this pathway is strongest in NH winter and weakest in NH summer (Figs. 7 and 15). The second exception takes place in the Asian lower troposphere during NH summer. The SHAF ozone is transported along the Somali jet, which is the second transport pathway, from eastern Africa near the equator to India (Fig. 16b), forming an African ozone maximum in the lower troposphere from the tropics to 15°N in NH summer (Fig. 5c). We find that the intensities of the ITCZ in Africa and the Somali jet can respectively explain approximately ~30% of the interannual variations in the transport of ozone from the southern hemispheric Africa to Asia in the two cases (Figs. 14a and 17).

This study provides an enhanced understanding of the source-receptor relationship of ozone transport from Africa to Asia. The findings on the transport routes from this study may also be applicable to other atmospheric pollutants with similar lifetimes, such as carbon monoxide. Our analysis is based on the simulations from the GEOS-Chem and HYSPLIT models, both of which have their own biases associated with emission inventories, parameterization schemes, and input data. The influences of African ozone can be further assessed by separating different emission sources.

Acknowledgments. We gratefully acknowledge that the GEOE-Chem model has been developed and managed by the Atmospheric Chemistry Modeling Group at Harvard University. The HYSPLIT (Hybrid Single-Particle Lagrangian Integrated Trajectory Model) model is developed by NOAA Air Resources Laboratory, driven by the *NCEP reanalysis data provided by NOAA/OAR/ESRL PSD, Boulder, Colorado, USA. The ozone sounding ozone sounde* data were ~~obtained~~acquired from the World Ozone and Ultraviolet Radiation Data Center (<http://www.woudc.org>) under the World Meteorological Organization. ~~This research is supported by the Natural Science~~

带格式的：左，缩进：首行缩进：0 字符

~~Foundation of China (41375140) and~~The TES ozone data are acquired from the NASA Langley Atmospheric Science Data Center. The NCEP/NCAR reanalysis and OLR data are from NOAA Earth System Research Laboratory. This research is supported by the Chinese Ministry of Science and Technology under the National Key Basic Research Development Program (2014CB441203, ~~2016YFA0600204~~) and the Natural Science Foundation of China (~~41375140 and~~ 91544230).

We are indeed grateful to the anonymous reviewers for their valuable and helpful reviews.

带格式的: 字体颜色: 文字 1

带格式的: 左

References

Aghedo, A. M., Schultz, M. G., and Rast, S.: The influence of African air pollution on regional and global tropospheric ozone, *Atmos. Chem. Phys.*, 7, 1193-1212, doi:10.5194/acp-7-1193-2007, 2007.

带格式的: 字体: 12 磅

带格式的: 左, 缩进: 左侧: 0 厘米, 悬挂缩进: 1 字符

Akritidis, D., Pozzer, A., Zanis, P., Tyrllis, E., Škerlak, B., Sprenger, M., and Lelieveld, J.: On the role of tropopause folds in summertime tropospheric ozone over the eastern Mediterranean and the Middle East, *Atmos. Chem. Phys.*, 16, 14025-14039, doi:10.5194/acp-16-14025-2016, 2016.

Albrecht, R. I., Goodman, S. J., Buechler, D. E., Blakeslee, R. J., and Christian, H. J.: Where are the lightning hotspots on Earth?, *Bull. Amer. Meteor. Soc.*, 97, 2051-2068, doi:10.1175/BAMS-D-14-00193.1, 2016.

Allen, D., Pickering, K., Duncan, B., and Damon, M.: Impact of lightning NO emissions on North American photochemistry as determined using the Global Modeling Initiative (GMI) model, *J. Geophys. Res.*, 115, D22301, doi:10.1029/2010JD014062, 2010.

~~An, Z., Wu, G., Li, J., Sun, Y., Liu, Y., Zhou, W., Cai, Y., Duan, A., Li, L., Mao, J., Cheng, H., Shi, Z., Tan, L., Yan, H., Ao, H., Chang, H., Feng, J.: Global Monsoon Dynamics and Climate Change, *Annu. Rev. Earth Planet. Sci.*, 43, 29-77, doi:10.1146/annurev-earth-060313-054623, 2015.~~

带格式的: 字体: 12 磅, 字体颜色: 自动设置

带格式的: 字体: 12 磅, 字体颜色: 自动设置

带格式的: 字体: 12 磅, 字体颜色: 自动设置

Anenberg, S. C., Horowitz, L. W., Tong, D. Q., and West, J. J.: An estimate of the global burden of anthropogenic ozone and fine particulate matter on premature human mortality using atmospheric modeling, *Environ. Health Persp.*, 118, 1189-1195, doi:10.1289/ehp.0901220, 2010.

带格式的: 字体: 12 磅

带格式的: 左, 缩进: 左侧: 0 厘米, 悬挂缩进: 1 字符

Avery, M., Westberg, D., Fuelberg, H., Newell, R., Anderson, B., Vay, S., Sachse, G., and Blake, D.: Chemical transport across the ITCZ in the central Pacific during an El Niño-Southern Oscillation cold phase event in March-April 1999, *J. Geophys. Res.*, 106, 32539-32553, doi:10.1029/2001JD000728, 2001.

带格式的: 字体: 12 磅

带格式的: 字体: 12 磅

~~Avery, M., Twohy, C., McCabe, D., Joiner, J., Severance, K., Atlas, E., Blake, D., Bui, T., Crounce, J.,~~

带格式的: 字体: 12 磅

~~and Dibb, J.: Convective distribution of tropospheric ozone and tracers in the Central American ITCZ region: Evidence from observations during TC4, J. Geophys. Res., 115, D00J21, doi:10.1029/2009JD013450, 2010.~~

带格式的: 字体: 12 磅, 字体颜色: 黑色

Avila, E. E., Bürgesser, R. E., Castellano, N. E., Collier, A. B., Compagnucci, R. H., and Hughes, A. R.: Correlations between deep convection and lightning activity on a global scale, J. Atmos. Sol-Terr. Phys., 72, 1114-1121, doi:10.1016/j.jastp.2010.07.019, 2010.

带格式的: 字体: 12 磅

带格式的: 左, 缩进: 左侧: 0 厘米, 悬挂缩进: 1 字符

~~Ben-Ami, Y., Koren, I., and Altaratz, O.: Patterns of North African dust transport over the Atlantic: winter vs. summer, based on CALIPSO first year data, Atmos. Chem. Phys., 9, 7867-7875, doi:10.5194/acp-9-7867-2009, 2009.~~

带格式的: 字体: 12 磅

Bey, I., Jacob, D. J., Logan, J. A., and Yantosca, R. M.: Asian chemical outflow to the Pacific in spring: Origins, pathways, and budgets, J. Geophys. Res., 106, 23073-23095, doi:10.1029/2001jd000807, 2001a.

带格式的: 字体: 12 磅

带格式的: 左, 缩进: 左侧: 0 厘米, 悬挂缩进: 1 字符

Bey, I., Jacob, D. J., Yantosca, R. M., Logan, J. A., Field, B. D., Fiore, A. M., Li, Q., Liu, H. Y., Mickley, L. J., and Schultz, M. G.: Global modeling of tropospheric chemistry with assimilated meteorology: Model description and evaluation, J. Geophys. Res., 106, 23073-23095, doi:10.1029/2001jd000806, 2001b.

Bouarar, I., Law, K. S., Pham, M., Liousse, C., Schlager, H., Hamburger, T., Reeves, C., Cammas, J.-P., Nédélec, P., and Szopa, S.: Emission sources contributing to tropospheric ozone over Equatorial Africa during the summer monsoon, Atmos. Chem. Phys., 11, 13395-13419, doi:10.5194/acp-11-13395-2011, 2011.

~~Chakraborty, T., Beig, G., Dentener, F. J., and Wild, O.: Atmospheric transport of ozone between Southern and Eastern Asia, Sci. Total Environ., 523, 28-39, doi:10.1016/j.scitotenv.2015.03.066, 2015.~~

带格式的: 字体: 12 磅, 字体颜色: 自动设置

~~Choi, H. D., Liu, H., Crawford, J. H., Considine, D. B., Allen, D. J., Duncan, B. N., Horowitz, L. W., Rodriguez, J. M., Strahan, S. E., Zhang, L., Liu, X., Damon, M. R., and Steenrod, S. D.: Global O₃-CO correlations in a chemistry and transport model during July-August: evaluation with TES satellite observations and sensitivity to input meteorological data and emissions, Atmos. Chem. Phys., 17, 8429-8452, doi:10.5194/acp-17-8429-2017, 2017.~~

带格式的: 字体: 12 磅

带格式的: 字体: 12 磅, 字体颜色: 自动设置

带格式的: 字体: 12 磅

带格式的: 字体: 12 磅, 字体颜色: 自动设置

带格式的: 字体: 12 磅

带格式的: 字体: 12 磅

带格式的: 字体: 12 磅

- Christian, H. J., Blakeslee, R. J., Boccippio, D. J., Boeck, W. L., Buechler, D. E., Driscoll, K. T., Goodman, S. J., Hall, J. M., Koshak, W. J., and Mach, D. M.: Global frequency and distribution of lightning as observed from space by the Optical Transient Detector, *J. Geophys. Res.*, 108, ACL 4-1-ACL 4-15, doi:10.1029/2002JD002347, 2003.
- Clain, G., Baray, J. L., Delmas, R., Diab, R., Bellevue, J. L. D., Keckhut, P., Posny, F., Metzger, J. M., and Cammas, J. P.: Tropospheric ozone climatology at two Southern Hemisphere tropical/subtropical sites, (Reunion Island and Irene, South Africa) from ozonesondes, LIDAR, and in situ aircraft measurements, *Atmos. Chem. Phys.*, 9, 1723-1734, doi:10.5194/acp-9-1723-2009, 2009.
- Collier, A. B., and Hughes, A. R.: Lightning and the African ITCZ, *J. Atmos. Sol-Terr. Phy.*, 73, 2392-2398, doi:10.1016/j.jastp.2011.08.010, 2011.
- Cooper, O., Moody, J., Parrish, D., Trainer, M., Ryerson, T., Holloway, J., Hübler, G., Fehsenfeld, F., and Evans, M.: Trace gas composition of midlatitude cyclones over the western North Atlantic Ocean: A conceptual model, *J. Geophys. Res.*, 107, 5-24, doi:10.1029/2001jd000901, 2002.
- Cooper, O., Parrish, D., Stohl, A., Trainer, M., Nédélec, P., Thouret, V., Cammas, J.-P., Oltmans, S., Johnson, B., and Tarasick, D.: Increasing springtime ozone mixing ratios in the free troposphere over western North America, *Nature*, 463, 344-348, doi:10.1038/nature08708, 2010.
- Cooper, O., Oltmans, S., Johnson, B., Brioude, J., Angevine, W., Trainer, M., Parrish, D., Ryerson, T., Pollack, I., and Cullis, P.: Measurement of western US baseline ozone from the surface to the tropopause and assessment of downwind impact regions, *J. Geophys. Res.*, 116, 898-908, doi:10.1029/2011JD016095, 2011.
- Cooper, O. R., Langford, A. O., Parrish, D. D., and Fahey, D. W.: Challenges of a lowered US ozone standard, *Science*, 348, 1096-1097, doi:10.1126/science.aaa5748, 2015.
- Derwent, R. G., Utembe, S. R., Jenkin, M. E., and Shallcross, D. E.: Tropospheric ozone production regions and the intercontinental origins of surface ozone over Europe, *Atmos. Environ.*, 112, 216-224, doi:10.1016/j.atmosenv.2015.04.049, 2015.

带格式的: 字体: 12 磅

带格式的: 左, 缩进: 左侧: 0 厘米, 悬挂缩进: 1 字符

~~Derwent, R. G., Parrish, D. D., Galbally, I. E., Stevenson, D. S., Doherty, R. M., Young, P. J., and Shallcross, D. E.: Interhemispheric differences in seasonal cycles of tropospheric ozone in the marine boundary layer: Observation model comparisons, *J. Geophys. Res.*, 121, 11075-11085, doi:10.1002/2016JD024836, 2016.~~

带格式的: 字体: 12 磅

带格式的: 字体: 12 磅

带格式的: 字体: 12 磅

~~Diedhiou, A., Janicot, S., Viltard, A., De Felice, P., and Laurent, H.: Easterly wave regimes and associated convection over West Africa and tropical Atlantic: results from the NCEP/NCAR and ECMWF reanalyses, *Clim. Dynam.*, 15, 795-822, 10.1007/s003820050316, 1999.~~

带格式的: 字体: 12 磅

~~Ding, Y., and Chan, J. C. L.: The East Asian summer monsoon: an overview, *Meteorol. Atmos. Phys.*, 89, 117-142, doi:10.1007/s00703-005-0125-z, 2005.~~

带格式的: 字体: 12 磅

~~Ding, Y., Liu, Y., Song, Y., and Zhang, J.: From MONEX to the Global Monsoon: A Review of Monsoon System Research, *Adv. Atmos. Sci.*, 32, 10-31, doi:10.1007/s00376-014-0008-7, 2015.~~

~~Doherty, O. M., Riemer, N., and Hameed, S.: Control of Saharan mineral dust transport to Barbados in winter by the Intertropical Convergence Zone over West Africa, *J. Geophys. Res.*, 117, 161-169, doi:10.1029/2012JD017767, 2012.~~

带格式的: 字体: 12 磅

带格式的: 左, 缩进: 左侧: 0 厘米, 悬挂缩进: 1 字符

Doherty, O. M., Riemer, N., and Hameed, S.: Role of the convergence zone over West Africa in controlling Saharan mineral dust load and transport in the boreal summer, *Tellus B*, 66, 759-763, doi:10.3402/tellusb.v66.23191, 2014.

Doherty, R., Wild, O., Shindell, D., Zeng, G., MacKenzie, I., Collins, W., Fiore, A. M., Stevenson, D., Dentener, F., and Schultz, M.: Impacts of climate change on surface ozone and intercontinental ozone pollution: A multi-model study, *J. Geophys. Res.*, 118, 3744-3763, doi:10.1002/jgrd.50266, 2013.

Doherty, R. M.: Atmospheric chemistry: Ozone pollution from near and far, *Nat. Geosci.*, 8, 664-665, doi:10.1038/ngeo2497, 2015.

~~Doherty, R. M., Orbe, C., Zeng, G., Plummer, D. A., Prather, M. J., Wild, O., Lin, M., Shindell, D. T., and Mackenzie, I. A.: Multi-model impacts of climate change on pollution transport from global emission source regions, *Atmos. Chem. Phys.*, 17, 14219-14237, doi:10.5194/acp-17-14219-2017, 2017.~~

带格式的: 字体: 12 磅

带格式的: 字体: 12 磅

带格式的: 字体: 12 磅

~~Draxler, R. R., and Hess, G.: An overview of the HYSPLIT_4 modelling system for trajectories, *Aust. Meteorol. Mag.*, 47, 295-308, 1998.~~

带格式的: 字体: 12 磅

带格式的: 左, 缩进: 左侧: 0 厘米, 悬挂缩进: 1 字符

~~Duncan, B. N., Martin, R. V., Staudt, A. C., Yevich, R., and Logan, J. A.: Interannual and seasonal~~

带格式的: 字体: 12 磅

带格式的: 字体: 12 磅

variability of biomass burning emissions constrained by satellite observations, *J. Geophys. Res.*, 108, ACH 11-1-ACH 11-22, doi:10.1029/2002JD002378, 2003.

带格式的: 字体: 12 磅, 字体颜色: 黑色

Fiore, A. M., Jacob, D. J., Bey, I., Yantosca, R. M., Field, B. D., Fusco, A. C., and Wilkinson, J. G.: Background ozone over the United States in summer: Origin, trend, and contribution to pollution episodes, *J. Geophys. Res.*, 107, ACH 11-1-ACH 11-25, doi:10.1029/2001JD000982, 2002.

带格式的: 字体: 12 磅

带格式的: 左, 缩进: 左侧: 0 厘米, 悬挂缩进: 1 字符

Fiore, A. M., Dentener, F., Wild, O., Cuvelier, C., Schultz, M., Hess, P., Textor, C., Schulz, M., Doherty, R., and Horowitz, L.: Multimodel estimates of intercontinental source-receptor relationships for ozone pollution, *J. Geophys. Res.*, 114, 83-84, doi:10.1029/2008JD010816, 2009.

Fleming, Z. L., Monks, P. S., and Manning, A. J.: Review: Untangling the influence of air-mass history in interpreting observed atmospheric composition, *Atmos. Res.*, 104, 1-39, doi:10.1016/j.atmosres.2011.09.009, 2012.

Fukutomi, Y., and Yasunari, T.: Structure and characteristics of submonthly-scale waves along the Indian Ocean ITCZ, *Clim. Dynam.*, 40, 1819-1839, doi:10.1007/s00382-012-1417-x, 2013.

Fukutomi, Y., and Yasunari, T.: Extratropical forcing of tropical wave disturbances along the Indian Ocean ITCZ, *J. Geophys. Res.*, 119, 1154-1171, doi:10.1002/2013JD020696, 2014.

Galmarini, S., Koffi, B., Solazzo, E., Keating, T., Hogrefe, C., Schulz, M., Benedictow, A., Griesfeller, J. J., Janssens-Maenhout, G., Carmichael, G., Fu, J., and Dentener, F.: Technical note: Coordination and harmonization of the multi-scale, multi-model activities HTAP2, AQMEII3, and MICS-Asia3: simulations, emission inventories, boundary conditions, and model output formats, *Atmos. Chem. Phys.*, 17, 1543-1555, doi:10.5194/acp-17-1543-2017, 2017.

带格式的: 字体: 12 磅

Garny, H., and Randel, W. J.: Transport pathways from the Asian monsoon anticyclone to the stratosphere, *Atmos. Chem. Phys.*, 16, 2703-2718, doi:10.5194/acp-16-2703-2016, 2016.

带格式的: 字体: 12 磅

带格式的: 左, 缩进: 左侧: 0 厘米, 悬挂缩进: 1 字符

Giglio, L., Randerson, J. T., and Werf, G. R.: Analysis of daily, monthly, and annual burned area using the fourth-generation global fire emissions database (GFED4), *J.*

- Geophys. Res., 118, 317-328, doi:10.1002/jgrg.20042, 2013.
- Guenther, A., Jiang, X., Heald, C., Sakulyanontvittaya, T., Duhl, T., Emmons, L., and Wang, X.: The Model of Emissions of Gases and Aerosols from Nature version 2.1 (MEGAN2.1): an extended and updated framework for modeling biogenic emissions, *Geosci. Model Dev.*, 5, 1471-1492, doi:10.5194/gmd-5-1471-2012, 2012.
- Gueroa, G., Bey, I., Attié J.-L., Martin, R., Cui, J., and Sprenger, M.: Impact of transatlantic transport episodes on summertime ozone in Europe, *Atmos. Chem. Phys.*, 6, 2057-2072, doi:10.5194/acp-6-2057-2006, 2006.
- Hack, J. J.: Parameterization of moist convection in the National Center for Atmospheric Research community climate model (CCM2), *J. Geophys. Res.*, 99, 5551-5568, doi:10.1029/93jd03478, 1994.
- ~~Halpern, D., and Woiceshyn, P. M.: Onset of the Somali Jet in the Arabian Sea during June 1997, *J. Geophys. Res.*, 104, 18041-18046, doi:10.1029/1999je900141, 1999.~~
- ~~Halpern, D., and Woiceshyn, P. M.: Somali Jet in the Arabian Sea, El Niño, and India Rainfall, *J. Climate*, 14, 434-441, doi:10.1175/1520-0442(2001)014<0434:sjitas>2.0.co;2, 2001.~~
- Hartley, D. E., and Black, R. X.: Mechanistic analysis of interhemispheric transport, *Geophys. Res. Lett.*, 22, 2945-2948, doi:10.1029/95gl02823, 1995.
- Hollaway, M. J., Arnold, S., Challinor, A. J., and Emberson, L.: Intercontinental trans-boundary contributions to ozone-induced crop yield losses in the Northern Hemisphere, *Biogeosciences*, 9, 271-292, doi:10.5194/bg-9-271-2012, 2012.
- Holloway, T., Sakurai, T., Han, Z., Ehlers, S., Spak, S. N., Horowitz, L. W., Carmichael, G. R., Streets, D. G., Hozumi, Y., and Ueda, H.: MICS-Asia II: Impact of global emissions on regional air quality in Asia, *Atmos. Environ.*, 42, 3543-3561, doi:10.1016/j.atmosenv.2007.10.022, 2008.
- HTAP: Hemispheric transport of air pollution 2010, United Nations, Dentener, F., Keating, T. and Akimoto, H. (eds.), New York and Geneva, 2010.
- Hu, Y., Li, D., and Liu, J.: Abrupt seasonal variation of the ITCZ and the Hadley circulation, *Geophys. Res. Lett.*, 34, 5407-5413, doi:10.1029/2007GL030950, 2007.
- Huang, R., Chen, J., Wang, L., and Lin, Z.: Characteristics, processes, and causes of the spatio-temporal variabilities of the East Asian monsoon system, *Adv. Atmos. Sci.*, 29,

带格式的: 字体: 12 磅

带格式的: 左, 缩进: 左侧: 0 厘米, 悬挂缩进: 1 字符

910-942, doi: 10.1007/s00376-012-2015-x, 2012.

Huang, M., Carmichael, G. R., Pierce, R. B., Jo, D. S., Park, R. J., Flemming, J., Emmons, L. K., Bowman, K. W., Henze, D. K., Davila, Y., Sudo, K., Jonson, J. E., Tronstad Lund, M., Janssens-Maenhout, G., Dentener, F. J., Keating, T. J., Oetjen, H., and Payne, V. H.: Impact of intercontinental pollution transport on North American ozone air pollution: an HTAP phase 2 multi-model study, *Atmos. Chem. Phys.*, 17, 5721-5750, doi:10.5194/acp-17-5721-2017, 2017.

Huntrieser, H., Heland, J., Schlager, H., Forster, C., Stohl, A., Aufmhoff, H., Arnold, F., Scheel, H., Campana, M., and Gilge, S.: Intercontinental air pollution transport from North America to Europe: Experimental evidence from airborne measurements and surface observations, *J. Geophys. Res.*, 110, 372-384, doi:10.1029/2004JD005045, 2005.

Ikeda, K., Tanimoto, H., Sugita, T., Akiyoshi, H., Kanaya, Y., Zhu, C., and Taketani, F.: Tagged tracer simulations of black carbon in the Arctic: transport, source contributions, and budget, *Atmos. Chem. Phys.*, 17, 10515-10533, doi:10.5194/acp-17-10515-2017, 2017.

Jaffe, D., McKendry, I., Anderson, T., and Price, H.: Six 'new' episodes of trans-Pacific transport of air pollutants, *Atmos. Environ.*, 37, 391-404, doi:10.1016/s1352-2310(02)00862-2, 2003.

Jiang, Z., Miyazaki, K., Worden, J. R., Liu, J. J., Jones, D. B. A., and Henze, D. K.: Impacts of anthropogenic and natural sources on free tropospheric ozone over the Middle East, *Atmos. Chem. Phys.*, 16, 6537-6546, doi:10.5194/acp-16-6537-2016, 2016.

~~Jones, C., Mahowald, N., and Luo, C.: The role of easterly waves on African desert dust transport, *J. Climate*, 16, 3617-3628, doi:10.1175/1520-0442(2003)016<3617:troewo>2.0.co;2, 2003.~~

~~Joseph, P., and Sijikumar, S.: Intraseasonal variability of the low-level jet stream of the Asian summer monsoon, *J. Climate*, 17, 1449-1458, doi:10.1175/1520-0442(2004)017<1449:ivotlj>2.0.co;2, 2004.~~

Kalnay, E., Kanamitsu, M., Kistler, R., Collins, W., Deaven, D., Gandin, L., Iredell, M., Saha, S., White, G., and Woollen, J.: The NCEP/NCAR 40-year reanalysis project, *Bull. Amer. Meteor. Soc.*, 77, 437-471,

带格式的: 字体: 12 磅
带格式的: 左, 缩进: 左侧: 0 厘米, 悬挂缩进: 1 字符

doi:10.1175/1520-0477(1996)077<0437:tnyrp>2.0.co;2, 1996.

Karamchandani, P., Long, Y., Pirovano, G., Balzarini, A., and Yarwood, G.:

Source-sector contributions to European ozone and fine PM in 2010 using AQMEII modeling data, Atmos. Chem. Phys., 17, 5643-5664, doi:10.5194/acp-17-5643-2017, 2017.

带格式的: 字体: 12 磅

Kim, M. J., Park, R. J., Ho, C.-H., Woo, J.-H., Choi, K.-C., Song, C.-K., and Lee, J.-B.:

Future ozone and oxidants change under the RCP scenarios, Atmos. Environ., 101, 103-115, doi:10.1016/j.atmosenv.2014.11.016, 2015.

带格式的: 字体: 12 磅

带格式的: 左, 缩进: 左侧: 0 厘米, 悬挂缩进: 1 字符

Knowland, K. E., Doherty, R. M., Hodges, K. I., and Ott, L. E.:

The influence of mid-latitude cyclones on European background surface ozone, Atmos. Chem. Phys., 17, 12421-12447, doi:10.5194/acp-17-12421-2017, 2017.

带格式的: 字体: 12 磅

带格式的: 字体: 12 磅

Koumoutsaris, S., Bey, I., Generoso, S., and Thouret, V.:

Influence of El Niño-Southern Oscillation on the interannual variability of tropospheric ozone in the northern midlatitudes, J. Geophys. Res., 113, D19301, doi:10.1029/2007JD009753, 2008.

带格式的: 字体: 12 磅

带格式的: 左, 缩进: 左侧: 0 厘米, 悬挂缩进: 1 字符

Kuhns, H., Green, M., and Etyemezian, V.: Big Bend Regional Aerosol and Visibility Observational (BRAVO) Study Emissions Inventory, 2003.

Lacis, A. A., Wuebbles, D. J., and Logan, J. A.: Radiative forcing of climate by changes in the vertical distribution of ozone, J. Geophys. Res., 95, 9971-9981, doi:10.1029/jd095id07p09971, 1990.

Lal, S., Venkataramani, S., Chandra, N., Cooper, O. R., Brioude, J., and Naja, M.:

Transport effects on the vertical distribution of tropospheric ozone over western India, J. Geophys. Res., 119, 10012-10026, doi:10.1002/2014JD021854, 2014.

Lefohn, A. S., Malley, C. S., Simon, H., Wells, B., Xu, X., Zhang, L., and Wang, T.:

Responses of human health and vegetation exposure metrics to changes in ozone concentration distributions in the European Union, United States, and China, Atmos. Environ., 152, 123-145, doi:10.1016/j.atmosenv.2016.12.025, 2017.

Lelieveld, J., and Dentener, F. J.: What controls tropospheric ozone?, J. Geophys. Res., 105, 3531-3551, doi:10.1029/1999jd901011, 2000.

Lewis, A., Evans, M., Methven, J., Watson, N., Lee, J., Hopkins, J., Purvis, R., Arnold, S., McQuaid, J., and Whalley, L.: Chemical composition observed over the

mid-Atlantic and the detection of pollution signatures far from source regions, J. Geophys. Res., 112, 815-838, doi:10.1029/2006JD007584, 2007.

Li, C., and Li, S.: Interannual Seesaw between the Somali and the Australian Cross-Equatorial Flows and its Connection to the East Asian Summer Monsoon, J. Climate, 27, 3966-3981, doi:10.1175/JCLI-D-13-00288.1, 2014a.

Li, X., Liu, J., Mauzerall, D. L., Emmons, L. K., Walters, S., Horowitz, L. W., and Tao, S.: Effects of trans-Eurasian transport of air pollutants on surface ozone concentrations over Western China, J. Geophys. Res., 119, 12338-12354, doi:10.1002/2014jd021936, 2014b.

~~Li, Z., Lau, W. K. M., Ramanathan, V., Wu, G., Ding, Y., Manoj, M. G., Liu, J., Qian, Y., Li, J., and Zhou, T.: Aerosol and monsoon climate interactions over Asia, Rev. Geophys., 54, 866-929, doi:10.1002/2015RG000500, 2016.~~

Liebmann, B., and Smith, C. A.: Description of a complete (interpolated) outgoing longwave radiation dataset, Bull. Amer. Meteor. Soc., 77, 1275-1277, 1996.

Lin, M., Horowitz, L. W., Payton, R., Fiore, A. M., and Tonnesen, G.: US surface ozone trends and extremes from 1980 to 2014: quantifying the roles of rising Asian emissions, domestic controls, wildfires, and climate, Atmos. Chem. Phys., 17, 2943-2970, doi:10.5194/acp-17-2943-2017, 2017.

Liu, H., Jacob, D. J., Chan, L. Y., Oltmans, S. J., Bey, I., Yantosca, R. M., Harris, J. M., Duncan, B. N., and Martin, R. V.: Sources of tropospheric ozone along the Asian Pacific Rim: An analysis of CO in the tropical troposphere using Aura satellite data and the GEOS-Chem model: ozonesonde observations, J. Geophys. Res., 107, ACH 3-1-ACH 3-19, doi:10.1029/2001JD002005, 2002.

Liu, J., Mauzerall, D., L., and Horowitz, L. W.: Analysis of seasonal and interannual variability of transpacific transport, J. Geophys. Res., 110, D04302, doi:10.1029/2004JD005207, 2005.

Liu, J., Logan, J. A., Jones, D. B., A., Livesey, N. J., Megretskaia, I., Carouge, C., and Nedelec, P.: insights into transport characteristics of the GEOS meteorological products, Atmos. Chem. Phys., 10, 12207-12232, doi:10.5194/acp-10-12207-2010, 2010.

带格式的: 字体: 12 磅

带格式的: 左

带格式的: 字体: 12 磅

带格式的: 字体: 12 磅

带格式的: 左, 缩进: 左侧: 0 厘米, 悬挂缩进: 1 字符

带格式的: 字体: 12 磅

带格式的: 字体: 12 磅, 字体颜色: 黑色

带格式的: 字体: 12 磅, 字体颜色: 黑色

带格式的: 字体: 12 磅

带格式的: 字体: 12 磅

Liu, J. J., Jones, D., Worden, J. R., Noone, D., Parrington, M., and Kar, J.: Analysis of the summertime buildup of tropospheric ozone abundances over the Middle East and North Africa as observed by the Tropospheric Emission Spectrometer instrument, *J. Geophys. Res.*, 114, 730-734, doi:10.1029/2008JD010993, 2009.

带格式的: 字体: 12 磅

带格式的: 左, 缩进: 左侧: 0 厘米, 悬挂缩进: 1 字符

Liu, J. J., Jones, D., Zhang, S., and Kar, J.: Influence of interannual variations in transport on summertime abundances of ozone over the Middle East, *J. Geophys. Res.*, 116, 999-1010, doi:10.1029/2011JD016188, 2011.

Long, M., Yantosca, R., Nielsen, J., Keller, C., da Silva, A., Sulprizio, M., Pawson, S., and Jacob, D.: Development of a grid-independent GEOS-Chem chemical transport model (v9-02) as an atmospheric chemistry module for Earth system models, *Geosci. Model. Dev.*, 8, 595-602, doi:10.5194/gmd-8-595-2015, 2015.

Marais, E. A., Jacob, D. J., Kurosu, T. P., Chance, K., Murphy, J. G., Reeves, C., Mills, G., Casadio, S., Millet, D. B., Barkley, M. P., Paulot, F., and Mao, J.: Isoprene emissions in Africa inferred from OMI observations of formaldehyde columns, *Atmos. Chem. Phys.*, 12, 6219-6235, doi:10.5194/acp-12-6219-2012, 2012.

Marais, E. A., Jacob, D. J., Guenther, A., Chance, K., Kurosu, T. P., Murphy, J. G., Reeves, C. E., and Pye, H. O. T.: Improved model of isoprene emissions in Africa using Ozone Monitoring Instrument (OMI) satellite observations of formaldehyde: implications for oxidants and particulate matter, *Atmos. Chem. Phys.*, 14, 7693-7703, doi:10.5194/acp-14-7693-2014, 2014.

带格式的: 字体: 12 磅

带格式的: 字体: 12 磅

带格式的: 字体: 12 磅

Martin, R. V., Sauvage, B., Folkins, I., Sioris, C. E., Boone, C., Bernath, P., and Ziemke, J.: Space-based constraints on the production of nitric oxide by lightning, *J. Geophys. Res.*, 112, D09309, doi:10.1029/2006JD007831, 2007.

带格式的: 字体: 12 磅

带格式的: 字体: 12 磅

L., Saunois, M., Attié, J., Thouret, V., and Stohl, A.: Tracing biomass burning plumes from the Southern Hemisphere during the AMMA 2006 wet season experiment, *Atmos. Chem. Phys.*, 8, 3951-3961, doi:10.5194/acp-8-3951-2008, 2008.

带格式的: 字体: 12 磅, 字体颜色: 黑色

带格式的: 字体: 12 磅

带格式的: 字体: 12 磅, 字体颜色: 黑色

Miyazaki, K., Eskes, H., Sudo, K., and Zhang, C.: Global lightning NO_x production estimated by an assimilation of multiple satellite data sets, *Atmos. Chem. Phys.*, 14, 3277-3305, doi:10.5194/acp-14-3277-2014, 2014.

带格式的: 字体: 12 磅

带格式的: 字体: 12 磅

带格式的: 左, 缩进: 左侧: 0 厘米, 悬挂缩进: 1 字符

Monks, P. S., Archibald, A., Colette, A., Cooper, O., Coyle, M., Derwent, R., Fowler, D., Granier, C., Law, K. S., and Mills, G.: Tropospheric ozone and its precursors from the urban to the global scale from air quality to short-lived climate forcer, *Atmos. Chem. Phys.*, 15, 8889-8973, doi:10.5194/acp-15-8889-2015, 2015.

Mounier, F., and Janicot, S.: Evidence of two independent modes of convection at intraseasonal timescale in the West African summer monsoon, *Geophys. Res. Lett.*, 31, 2876-2877, doi:10.1029/2004GL020665, 2004.

Myhre, G., Shindell, D., Br éon, F.-M., Collins, W., Fuglestedt, J., Huang, J., Koch, D., Lamarque, J.-F., Lee, D., Mendoza, B., Nakajima, T., Robock, A., Stephens, G., Takemura, T., and Zhang, H.: Anthropogenic and Natural Radiative Forcing, In: *Climate Change 2013: The Physical Science Basis, Contribution of Working Group I to the Fifth Assessment Report of the Intergovernmental Panel on Climate Change*, Cambridge University Press, Cambridge, United Kingdom and New York, NY, USA, 659-740, 2013.

Nagashima, T., Ohara, T., Sudo, K., and Akimoto, H.: The relative importance of various source regions on East Asian surface ozone, *Atmos. Chem. Phys.*, 10, 11305-11322, doi:10.5194/acp-10-11305-2010, 2010.

Nassar, R., Logan, J. A., Worden, H. M., Megretskaia, I. A., Bowman, K. W., Osterman, G. B., Thompson, A. M., Tarasick, D. W., Austin, S., Claude, H., Dubey, M. K., Hocking, W. K., Johnson, B. J., Joseph, E., Merrill, J., Morris, G. A., Newchurch, M., Oltmans, S. J., Posny, F., Schmidlin, F. J., V ömel, H., Whiteman, D. N., and Witte, J. C.: Validation of Tropospheric Emission Spectrometer (TES) nadir ozone profiles using ozonesonde measurements, *J. Geophys. Res.*, 113, D15S17, doi:10.1029/2007JD008819, 2008.

Neu, J. L., Flury, T., Manney, G. L., Santee, M. L., Livesey, N. J., and Worden, J.: Tropospheric ozone variations governed by changes in stratospheric circulation, *Nat. Geosci.*, 7, 340-344, doi:10.1038/NGEO2138, 2014.

~~Nicholson, S. E., and Grist, J. P.: The seasonal evolution of the atmospheric circulation over West Africa and equatorial Africa, *J. Climate*, 16, 1013-1030, doi:10.1175/1520-0442(2003)016<1013:tseota>2.0.co;2, 2003.~~

带格式的: 字体: 12 磅

带格式的: 字体: 12 磅, 字体颜色: 黑色

带格式的: 字体: 12 磅, 字体颜色: 黑色

带格式的: 字体: 12 磅, 字体颜色: 黑色

带格式的: 字体: 12 磅, 字体颜色: 黑色

带格式的: 字体: 12 磅

带格式的: 左, 缩进: 左侧: 0 厘米, 悬挂缩进: 1 字符

~~Nicholson, S. E.:~~ The intensity, location and structure of the tropical rainbelt over west Africa as factors in interannual variability, *Int. J.Climatol.*, 28, 1775-1785, doi:10.1002/joc.1507, 2008.

带格式的: 字体: 12 磅

带格式的: 左

Nicholson, S. E.: A revised picture of the structure of the “monsoon” and land ITCZ over West Africa, *Clim. Dynam.*, 32, 1155-1171, doi:10.1007/s00382-008-0514-3, 2009.

带格式的: 左, 缩进: 左侧: 0 厘米, 悬挂缩进: 1 字符

~~Nützel,~~ Nicholson, S. E.: The West African Sahel: A Review of Recent Studies on the Rainfall Regime, ~~M., Dameris, M., and Gamy, H.: Movement, drivers~~ Its Interannual Variability, *ISRN Meteorology*, 2013, 32, doi:10.1155/2013/453521, 2013.

带格式的: 字体: 12 磅, 字体颜色: 黑色

带格式的: 字体: 12 磅

Nicholson, S. E.: Climate and bimodality of the South Asian High climatic variability of rainfall over eastern Africa, *Rev. Geophys.*, 55, 590-635, doi:10.1002/2016RG000544, 2017.

带格式的: 字体: 12 磅

Nopmongcol, U., Liu, Z., Stoeckenius, T., and Yarwood, G.: Modeling intercontinental transport of ozone in North America with CAMx for the Air Quality Model Evaluation International Initiative (AQMEII) Phase 3, *Atmos. Chem. Phys.*, ~~+6,~~ 17, 9931-9943, doi:10.5194/acp-~~16-14755-2016,~~ 201617-9931-2017, 2017.

带格式的: 左

带格式的: 字体: 12 磅

带格式的: 字体: 12 磅

带格式的: 字体: 12 磅

Olivier, J.G.J. and J.J.M. Berdowski, Global emissions sources and sinks. In: Berdowski, J., Guicherit, R. and B.J. Heij (eds.) *The Climate System*, pp. 33-78. A. A. Balkema Publishers/Swets & Zeitlinger Publishers, Lisse, The Netherlands., 2001

带格式的: 左, 缩进: 左侧: 0 厘米, 悬挂缩进: 1 字符

Ott, L. E., Pickering, K. E., Stenchikov, G. L., Allen, D. J., Decaria, A. J., Ridley, B., Lin, R. F., Lang, S., and Tao, W. K.: Production of lightning NOx and its vertical distribution calculated from three-dimensional cloud-scale chemical transport model simulations, *J. Geophys. Res.*, 115, 288-303, doi:10.1029/2009JD011880, 2010.

Philip, S., Martin, R. V., and Keller, C. A.: Sensitivity of chemistry-transport model simulations to the duration of chemical and transport operators: a case study with GEOS-Chem v10-01, *Geosci. Model. Dev.*, 9, 1683-1695, doi:10.5194/gmd-9-1683-2016, 2016.

Pickering, K. E., Wang, Y., Tao, W. K., Price, C., and Müller, J. F.: Vertical distributions of lightning NOx for use in regional and global chemical transport models, *J. Geophys. Res.*, 103, 31203-31216, doi:10.1029/98jd02651, 1998.

- Piketh, S. J. and Walton, N. W.: Characteristics of Atmospheric Transport of Air Pollution for Africa, In: Stohl, A., ed., Intercontinental Transport of Air Pollution, Springer Berlin Heidelberg, 173-197, 2004.
- Pochanart, P., Akimoto, H., Kajii, Y., and Sukasem, P.: Carbon monoxide, regional - scale transport, and biomass burning in tropical continental Southeast Asia: Observations in rural Thailand, *J. Geophys. Res.*, 108, 1337-1352, doi:doi:10.1029/2002JD003360, 2003.
- Pochanart, P., Wild, O., and Akimoto, H.: Air pollution import to and export from East Asia, *Air Pollution*, 99-130, 2004.
- Pulles, T., Bolscher, M. V. H., Brand, R., and Visschedijk, A.: Assessment of Global Emissions from Fuel Combustion in the Final Decades of the 20th Century, TNO report A-R0132/B, 2007.
- Raper, J. L., Kleb, M. M., Jacob, D. J., Davis, D. D., Newell, R. E., Fuelberg, H. E., Bendura, R. J., Hoell, J. M., and McNeal, R. J.: Pacific Exploratory Mission in the Tropical Pacific- PEM-Tropics B, March-April 1999, *J. Geophys. Res.*, 106, 32401-32425, doi:10.1029/2000JD900833, 2001.
- ~~Rastigejev, Y., Park, R., Brenner, M. P., and Jacob, D. J.: Resolving intercontinental pollution plumes in global models of atmospheric transport, *J. Geophys. Res.*, 115, D02302, doi:10.1029/2009JD012568, 2010.~~
- Ridder, T., Gerbig, C., Notholt, J., Rex, M., Schrems, O., Warneke, T., and Zhang, L.: Ship-borne FTIR measurements of CO and O₃ in the Western Pacific from 43 °N to 35 °S: an evaluation of the sources, *Atmos. Chem. Phys.*, 12, 815-828, doi:10.5194/acp-12-815-2012, 2012.
- Rodríguez, S., Cuevas, E., Prospero, J., Alastuey, A., Querol, X., López-Solano, J., García, M., and Alonso-Pérez, S.: Modulation of Saharan dust export by the North African dipole, *Atmos. Chem. Phys.*, 15, 7471-7486, doi:10.5194/acp-15-7471-2015, 2015.
- Sauvage, B., Thouret, V., Cammas, J.-P., Gheusi, F., Athier, G., and Nédélec, P.: Tropospheric ozone over Equatorial Africa: regional aspects from the MOZAIC data, *Atmos. Chem. Phys.*, 5, 311-335, doi:10.5194/acp-5-311-2005, 2005.

带格式的: 字体: 12 磅

带格式的: 左, 缩进: 左侧: 0 厘米, 悬挂缩进: 1 字符

Sekiya, T., and Sudo, K.: Role of meteorological variability in global tropospheric ozone during 1970-2008, *J. Geophys. Res.*, 117, D18303, doi:10.1029/2012JD018054, 2012.

Sekiya, T., and Sudo, K.: Roles of transport and chemistry processes in global ozone change on interannual and multidecadal time scales, *J. Geophys. Res.*, 119, 4903-4921, doi:10.1002/2013JD020838, 2014.

Stein, A. F., Draxler, R. R., Rolph, G. D., Stunder, B. J. B., Cohen, M. D., and Ngan, F.: NOAA's HYSPLIT Atmospheric Transport and Dispersion Modeling System, *Bull. Amer. Meteor. Soc.*, 96, 2059-2077, doi:10.1175/bams-d-14-00110.1, 2015.

~~Streets, D. G., Bond, T. C., Carmichael, G. R., Fernandes, S. D., He, D., Klimont, Z., Nelson, S. M., Tsai, N. Y., and Wang, M. Q.: An inventory of gaseous and primary aerosol emissions in Asia in the year 2000, *J. Geophys. Res.*, 108, GTE 30-1-GTE 30-23, doi:10.1029/2002JD003093, 2003.~~

带格式的: 字体: 12 磅

~~Streets, D. G., Zhang, Q., Wang, L., He, K., Hao, J., Wu, Y., Tang, Y., and Carmichael, G. R.: Revisiting China's CO emissions after the Transport and Chemical Evolution over the Pacific (TRACE-P) mission: Synthesis of inventories, atmospheric modeling, and observations, *J. Geophys. Res.*, 111, D14306, doi:10.1029/2006JD007118, 2006.~~

带格式的: 字体: 12 磅

Sudo, K., and Akimoto, H.: Global source attribution of tropospheric ozone: Long-range transport from various source regions, *J. Geophys. Res.*, 112, D12302, doi:10.1029/2006JD007992, 2007.

带格式的: 字体: 12 磅

带格式的: 左, 缩进: 左侧: 0 厘米, 悬挂缩进: 1 字符

Sultan, B., and Janicot, S.: Abrupt shift of the ITCZ over West Africa and intra-seasonal variability, *Geophys. Res. Lett.*, 27, 3353-3356, doi:10.1029/1999gl011285, 2000.

Suzuki, T.: Seasonal variation of the ITCZ and its characteristics over central Africa, *Theor. Appl. Climatol.*, 103, 39-60, doi:10.1007/s00704-010-0276-9, 2011.

Thompson, A. M.: Intercontinental Transport of Ozone from Tropical Biomass Burning, In: Stohl, A., ed., *Intercontinental Transport of Air Pollution*, Springer Berlin Heidelberg, 225-254, 2004.

Thompson, A. M., Miller, S. K., Tilmes, S., Kollonige, D. W., Witte, J. C., Oltmans, S. J., Johnson, B. J., Fujiwara, M., Schmidlin, F., and Coetzee, G.: Southern Hemisphere Additional Ozonesondes (SHADOZ) ozone climatology (2005-2009): Tropospheric and tropical tropopause layer (TTL) profiles with comparisons to

OMI-based ozone products, *J. Geophys. Res.*, 117, D23301,
doi:10.1029/2011JD016911, 2012.

Thompson, A. M., Balashov, N. V., Witte, J., Coetzee, J., Thouret, V., and Posny, F.:
Tropospheric ozone increases over the southern Africa region: bellwether for rapid
growth in Southern Hemisphere pollution^{2,2}, *Atmos. Chem. Phys.*, 14, 9855-9869,
doi:10.5194/acp-14-9855-2014, 2014.

带格式的: 字体: 12 磅

~~Tie, X., Guenther, A., and Holland, E.: Biogenic methanol and its impacts on tropospheric oxidants,
Geophys. Res. Lett., 30, ASC 3-1 ASC 3-3, doi:10.1029/2003GL017167, 2003.~~

带格式的: 字体: 12 磅

带格式的: 字体: 12 磅

Van der Werf, G. R., Randerson, J. T., Giglio, L., Collatz, G. J., Mu, M., Kasibhatla, P.
S., Morton, D. C., Defries, R. S., Jin, Y., and Leeuwen, T. T. V.: Global fire emissions
and the contribution of deforestation, savanna, forest, agricultural, and peat fires
(1997–2009), *Atmos. Chem. Phys.*, 10, 16153-16230,
doi:10.5194/acp-10-11707-2010, 2010.

带格式的: 字体: 12 磅

带格式的: 左, 缩进: 左侧: 0 厘米, 悬挂缩进: 1 字符

Verstraeten, W. W., Neu, J. L., Williams, J. E., Bowman, K. W., Worden, J. R., and
Boersma, K. F.: Rapid increases in tropospheric ozone production and export from
China, *Nat. Geosci.*, 8, 690-695, doi:10.1038/NGEO2493, 2015.

Vestreng, V., and Klein, H.: Emission data reported to UNECE/EMEP: Quality
assurance and trend analysis & Presentation of WebDab, MSC-W Status Report
2002, Norwegian Meteorological Institute, Oslo Norway, July 2002.

Vogel, B., Günther, G., Müller, R., Groß, J.-U., Hoor, P., Krämer, M., Müller, S., Zahn,
A., and Riese, M.: Fast transport from Southeast Asia boundary layer sources to
northern Europe: rapid uplift in typhoons and eastward eddy shedding of the Asian
monsoon anticyclone, *Atmos. Chem. Phys.*, 14, 12745-12762,
doi:10.5194/acp-14-12745-2014, 2014.

Waliser, D. E., and Gautier, C.: A satellite-derived climatology of the ITCZ, *J. Climate*,
6, 2162-2174, doi:10.1175/1520-0442(1993)006<2162:asdcot>2.0.co;2, 1993.

Waliser, D. E., Graham, N. E., and Gautier, C.: Comparison of the highly reflective
cloud and outgoing longwave radiation datasets for use in estimating tropical deep
convection, *J. Climate*, 6, 331-353,
doi:10.1175/1520-0442(1993)006<0331:cothrc>2.0.co;2, 1993.

~~Wang, Y., Logan, J. A., and Jacob, D. J.: Global simulation of tropospheric O₃, NO_x, hydrocarbon chemistry: 2. Model evaluation and global ozone budget, J. Geophys. Res., 103, 10727-10755, doi:10.1029/98jd00157, 1998.~~

带格式的: 字体: 12 磅

~~Wang, Y., Zhang, Y., Hao, J., and Luo, M.: Seasonal and spatial variability of surface ozone over China: contributions from background and domestic pollution, Atmos. Chem. Phys., 11, 3511-3525, doi:10.5194/acp-11-3511-2011, 2011.~~

带格式的: 左

带格式的: 字体: 12 磅

~~Wild, O., Law, K. S., McKenna, D. S., Bandy, B. J., Penkett, S. A., and Pyle, J. A.: Photochemical trajectory modeling studies of the North Atlantic region during August 1993, J. Geophys. Res., 101, 29269-29288, doi:10.1029/96jd00837, 1996.~~

带格式的: 左, 缩进: 左侧: 0 厘米, 悬挂缩进: 1 字符

~~Wild, O., Pochanart, P., and Akimoto, H.: Trans-Eurasian transport of ozone and its precursors, J. Geophys. Res., 109, D11302, doi:10.1029/2003JD004501, 2004.~~

~~Williams, J., Scheele, M., Van Velthoven, P., Cammas, J.-P., Thouret, V., Galy-Lacaux, C., and Volz-Thomas, A.: The influence of biogenic emissions from Africa on tropical tropospheric ozone during 2006: a global modeling study, Atmos. Chem. Phys., 9, 5729-5749, doi:10.5194/acp-9-5729-2009, 2009.~~

~~Wu, G., Liu, Y., Bian, H., Bao, Q., Duan, A., and Jin, F. F.: Thermal Controls on the Asian Summer Monsoon, Sci. Rep., 2, 404, doi:10.1038/srep00404, 2012.~~

带格式的: 字体: 12 磅

~~Wu, G., Duan, A., Liu, Y., Mao, J., Ren, R., Bao, Q., He, B., Liu, B., and Hu, W.: Tibetan Plateau climate dynamics: recent research progress and outlook, Natl. Sci. Rev., 2, 100-116, doi:10.1093/nsr/nwu045, 2015.~~

带格式的: 字体: 12 磅

带格式的: 字体: 12 磅, 字体颜色: 黑色

带格式的: 字体: 12 磅

~~Xie, S.-P.: The shape of continents, air-sea interaction, and the rising branch of the Hadley circulation, in: The Hadley Circulation: Present, Past and Future, Springer, 121-152, 2004.~~

带格式的: 字体: 12 磅

带格式的: 左, 缩进: 左侧: 0 厘米, 悬挂缩进: 1 字符

~~Yevich, R., and Logan, J. A.: An assessment of biofuel use and burning of agricultural waste in the developing world, Global Biogeochem. Cy., 17, 1095, doi:10.1029/2002GB001952, 2003.~~

~~Žagar, N., Skok, G., and Tribbia, J.: Climatology of the ITCZ derived from ERA Interim reanalyses, J. Geophys. Res., 116, D15103, doi:10.1029/2011JD015695, 2011.~~

~~Zare, A., Christensen, J. H., Gross, A., Irannejad, P., Glasius, M., and Brandt, J.:~~

Quantifying the contributions of natural emissions to ozone and total fine PM concentrations in the Northern Hemisphere, *Atmos. Chem. Phys.*, 14, 2735-2756, doi:10.5194/acp-14-2735-2014, 2014.

Zhang, G. J., and McFarlane, N. A.: Sensitivity of climate simulations to the parameterization of cumulus convection in the Canadian climate centre general circulation model, *Atmos. Ocean.*, 33, 407-446, doi:10.1080/07055900.1995.9649539, 1995.

Zhang, Y., Li, T., Wang, B., and Wu, G.: Onset of the Summer Monsoon over the Indochina Peninsula: Climatology and Interannual Variations, *J. Climate*, 15, 3206-3221, doi:10.1175/1520-0442(2002)015<3206:eotsmo>2.0.co;2, 2002. L., Li, Q. B., Jin, J., Liu, H., Livesey, N., Jiang, J. H., Mao, Y., Chen, D., Luo, M., and Chen, Y.: Impacts of 2006 Indonesian fires and dynamics on tropical upper tropospheric carbon monoxide and ozone, *Atmos. Chem. Phys.*, 11, 10929-10946, doi:10.5194/acp-11-10929-2011, 2011.

带格式的: 字体: 12 磅

Zhang, L., Jacob, D. J., Boersma, K. F., Jaffe, D. A., Olson, J. R., Bowman, K. W., Worden, J. R., Thompson, A. M., Avery, M. A., Cohen, R. C., Dibb, J. E., Flock, F. M., Fuelberg, H. E., Huey, L. G., McMillan, W. W., Singh, H. B., and Weinheimer, A. J.: Transpacific transport of ozone pollution and the effect of recent Asian emission increases on air quality in North America: an integrated analysis using satellite, aircraft, ozonesonde, and surface observations, *Atmos. Chem. Phys.*, 8, 6117-6136, doi:10.5194/acp-8-6117-2008, 2008.

Zhang, Q., Streets, D. G., Carmichael, G. R., He, K. B., Huo, H., Kannari, A., Klimont, Z., Park, I. S., Reddy, S., Fu, J. S., Chen, D., Duan, L., Lei, Y., Wang, L. T., and Yao, Z. L.: Asian emissions in 2006 for the NASA INTEX-B mission, *Atmos. Chem. Phys.*, 9, 5131-5153, doi:10.5194/acp-9-5131-2009, 2009.

带格式的: 字体: 12 磅

Zhao, T., Gong, S., Zhang, X., and McKendry, I.: Modeled size-segregated wet and dry deposition budgets of soil dust aerosol during ACE-Asia 2001: Implications for trans-Pacific transport, *J. Geophys. Res.*, 108, 420-424, doi:10.1029/2002JD003363, 2003.

带格式的: 字体: 12 磅

带格式的: 左, 缩进: 左侧: 0 厘米, 悬挂缩进: 1 字符

Zhao, T., Gong, S., Huang, P., and Lavoué D.: Hemispheric transport and influence of meteorology on

~~global aerosol climatology, Atmos. Chem. Phys., 12, 7609-7624, doi:10.5194/acp-12-7609-2012, 2012.~~

带格式的: 字体: 12 磅

Zhu, Y.: Variations of the summer Somali and Australia cross-equatorial flows and the implications for the Asian summer monsoon, Adv. Atmos. Sci., 29(3), 509-518, doi:10.1007/s00376-011-1120-6, 2012.

带格式的: 字体: 12 磅

带格式的: 左, 缩进: 左侧: 0 厘米, 悬挂缩进: 1 字符

Zhu, B., Hou, X., and Kang, H.: Analysis of the seasonal ozone budget and the impact of the summer monsoon on the northeastern Qinghai-Tibetan Plateau, J. Geophys. Res., 121, 2029-2042, doi:10.1002/2015JD023857, 2016.

Zhu, J., Liao, H., Mao, Y., Yang, Y., and Jiang, H.: Interannual variation, decadal trend, and future change in ozone outflow from East Asia, Atmos. Chem. Phys., 17, 3729-3747, doi:10.5194/acp-17-3729-2017, 2017a.

Zhu, Y., Liu, J., Wang, T., Zhuang, B., Han, H., Wang, H., Chang, Y., and Ding, K.: The impacts of meteorology on the seasonal and interannual variabilities of ozone transport from North America to East Asia, J. Geophys. Res., 122, doi:10.1002/2017JD026761, 2017b.

带格式的: 字体颜色: 自动设置

带格式的: 左, 段落间距段后: 10 磅, 行距: 多倍行距 1.15 字行